Multi-scale, multi-physics structure formation simulations

Volker Springel

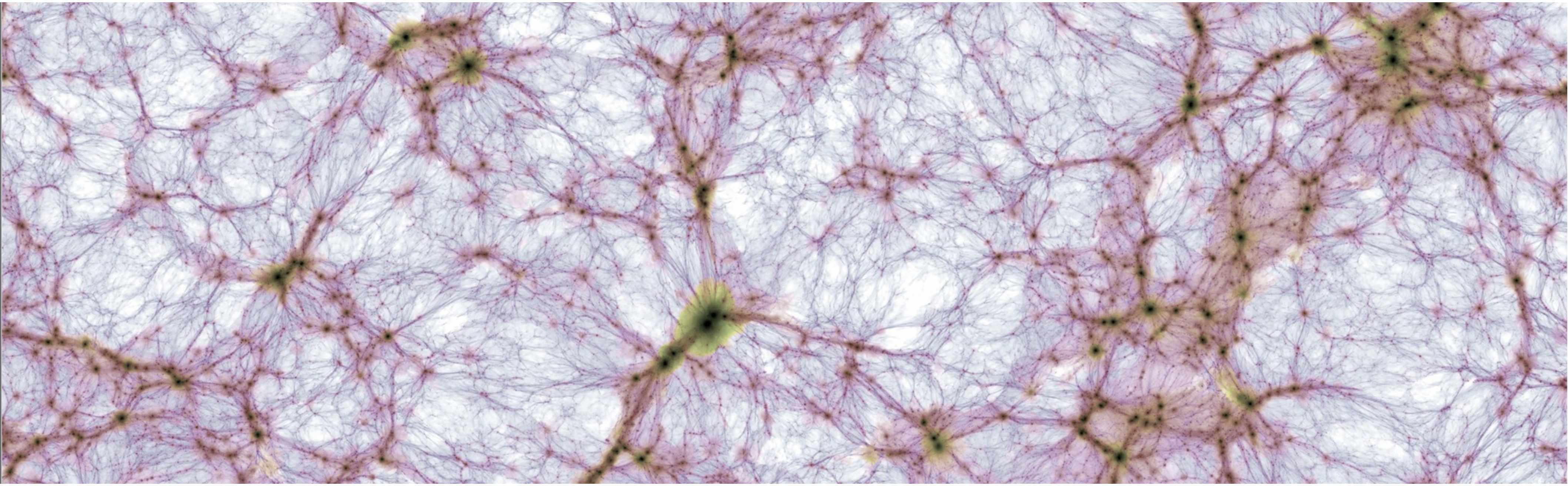

- The Next Generation Illustris Simulations (IllustrisTNG)
- The role of black holes in galaxy formation simulations
- Modelling directions: Magnetic fields, cosmic rays, radiation hydro, ...

Max-Planck-Institute for Astrophysics

Universität Heidelberg

Heidelberg Institute for Theoretical Studies

HITS

Stars, Planets, and Galaxies
Harnack Haus
Berlin, April 2018

The multifaceted need for **feedback**

Star formation in the ISM is surprisingly inefficient

THE GAS CONSUMPTION TIMESCALE OF STAR FORMATION

depletion time:

$$t_{\rm dep} \equiv M_{\rm gas}/\dot{M}_*$$

gravitational free-fall time:

$$t_{\rm ff} = \sqrt{\frac{3\pi}{32G\rho}}$$

dimensionless "efficiency" of star formation:

$$\epsilon_{\rm ff} \equiv \frac{t_{\rm ff}}{t_{\rm dep}}$$

observed is:

$$\dot{\Sigma}_\star \simeq \epsilon_{\rm ff}\frac{\Sigma_{\rm H_2}}{t_{\rm ff}}$$

$$\epsilon_{\rm ff} \sim 0.01$$

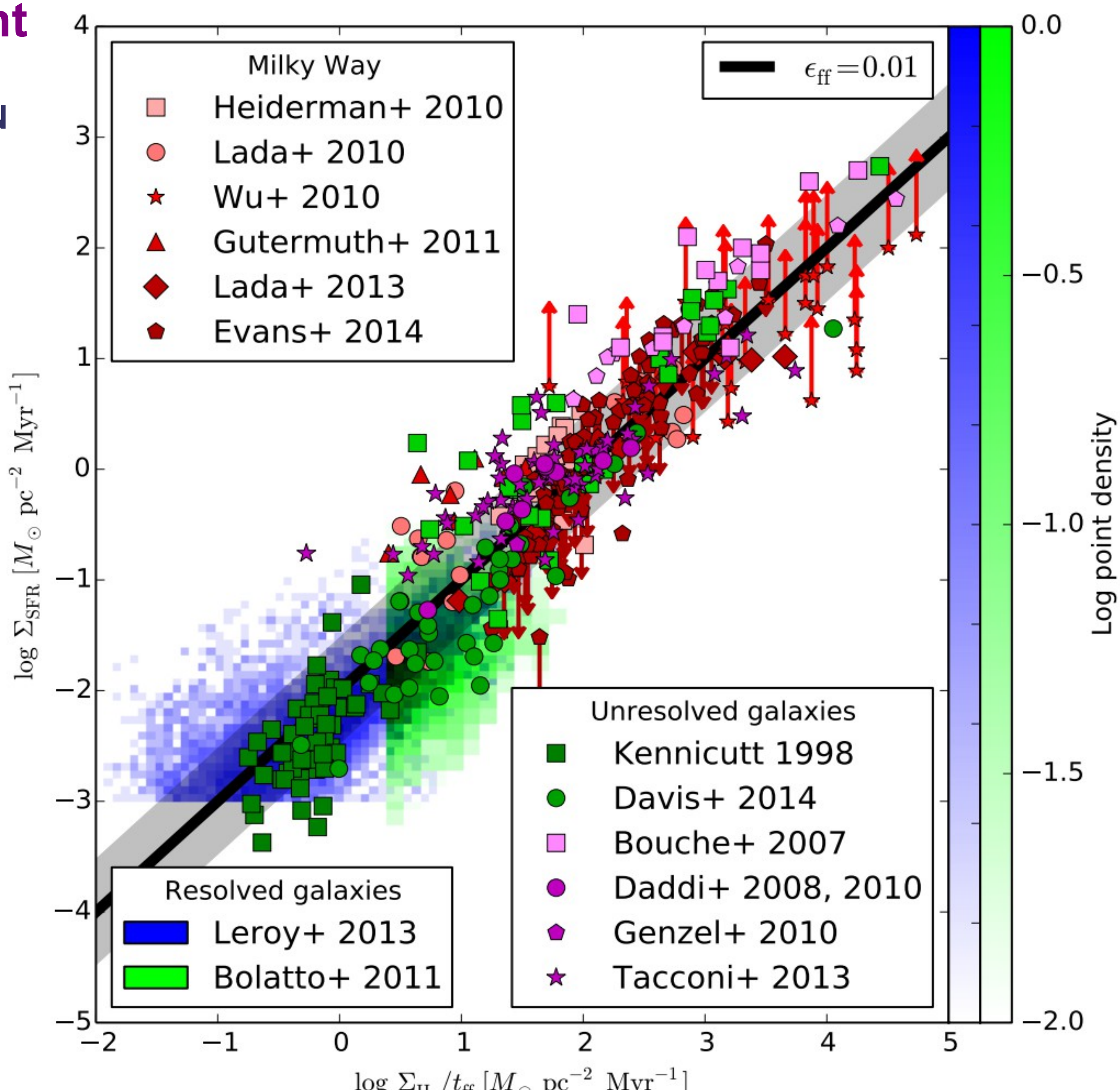

Krumholz et al. (2014)

Abundance matching gives the expected halo mass – stellar mass relation in ΛCDM

MODULATION OF GLOBAL STAR FORMATION EFFICIENCY AS A FUNCTION OF HALO MASS

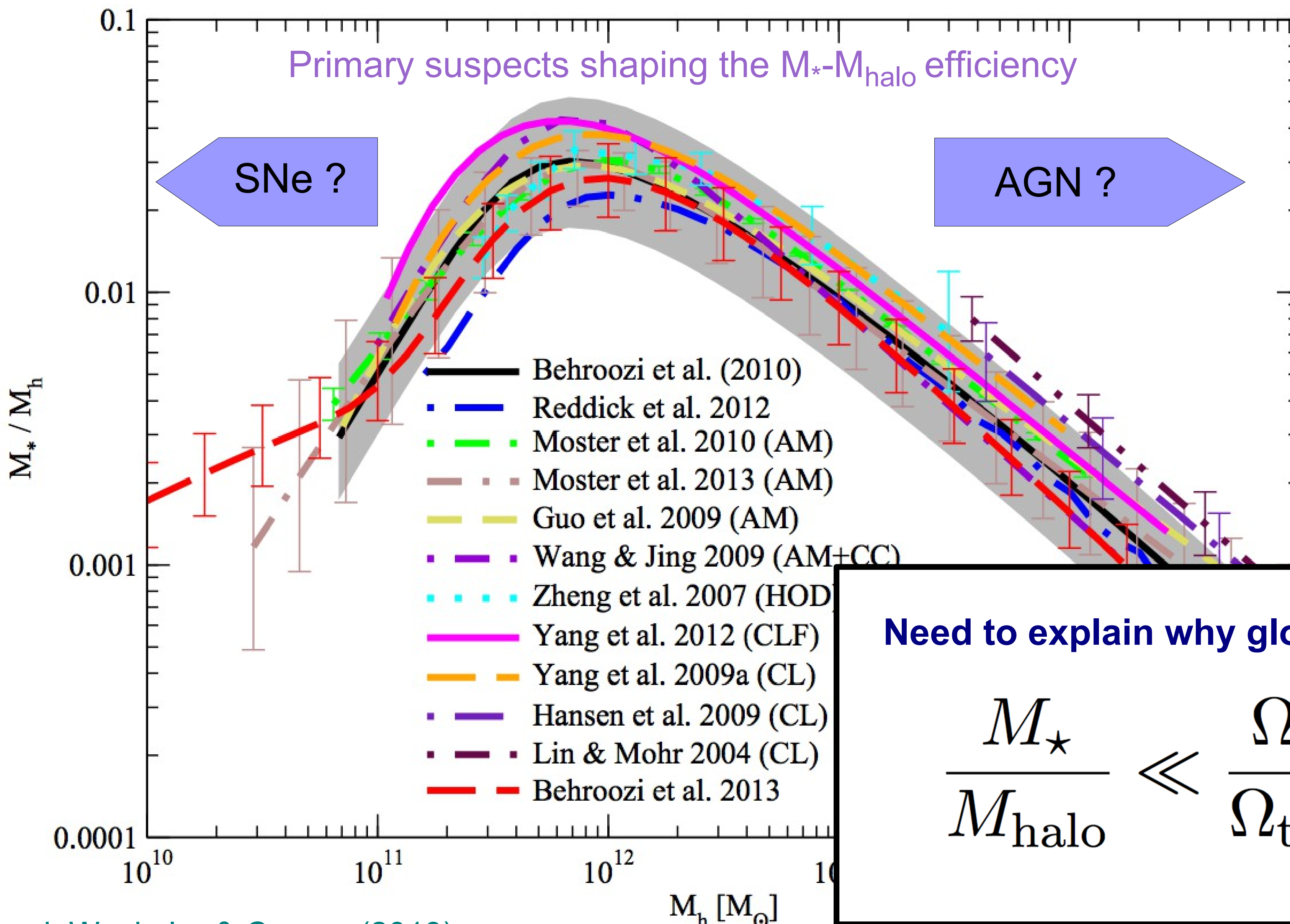

Need to explain why globally:

$$\frac{M_\star}{M_{\rm halo}} \ll \frac{\Omega_b}{\Omega_{\rm tot}}$$

Behroozi, Wechsler & Conroy (2013)

Black hole energetics suggests that they could influence the evolution of galaxies

COMPARING SUPERNOVA AND BLACK HOLE ENERGIES

quasars / AGN

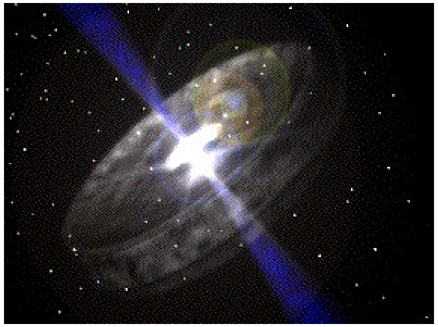

What's the connection?

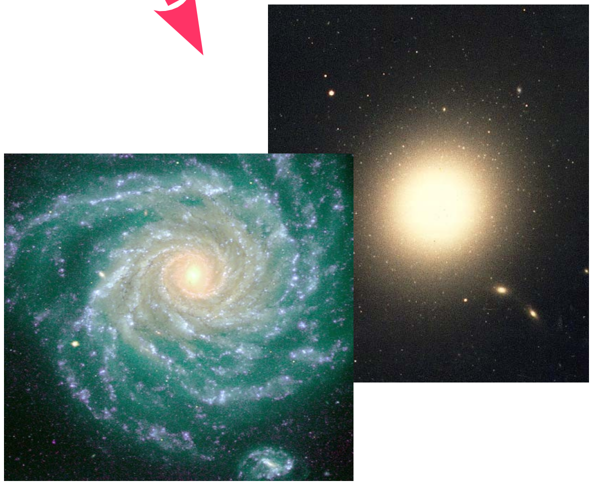

galaxies

Quasars release plenty of energy

$$L_Q \sim 10^{12}\, L_\odot \qquad t_Q \sim 10^7 - 10^8\,\mathrm{yr}$$

$$E_Q \sim 10^{60} - 10^{61}\,\mathrm{erg}$$

a billion supernovae !

But how does AGN energy couple to halo gas?

Total available feedback energy from BHs is comparable to that of supernovae

$$\rho_{\rm BH} \simeq 0.001\,\rho_\star$$

$$E_{\rm BH}/V \simeq 0.1\,\rho_{\rm BH}\,c^2$$

$$E_{\rm SN}/V \simeq \frac{10^{51}\,\mathrm{erg}}{100\,\mathrm{M}_\odot}\,\rho_\star$$

$$\frac{E_{\rm BH}}{E_{\rm SN}} \simeq 1.8$$

The dynamic range challenge

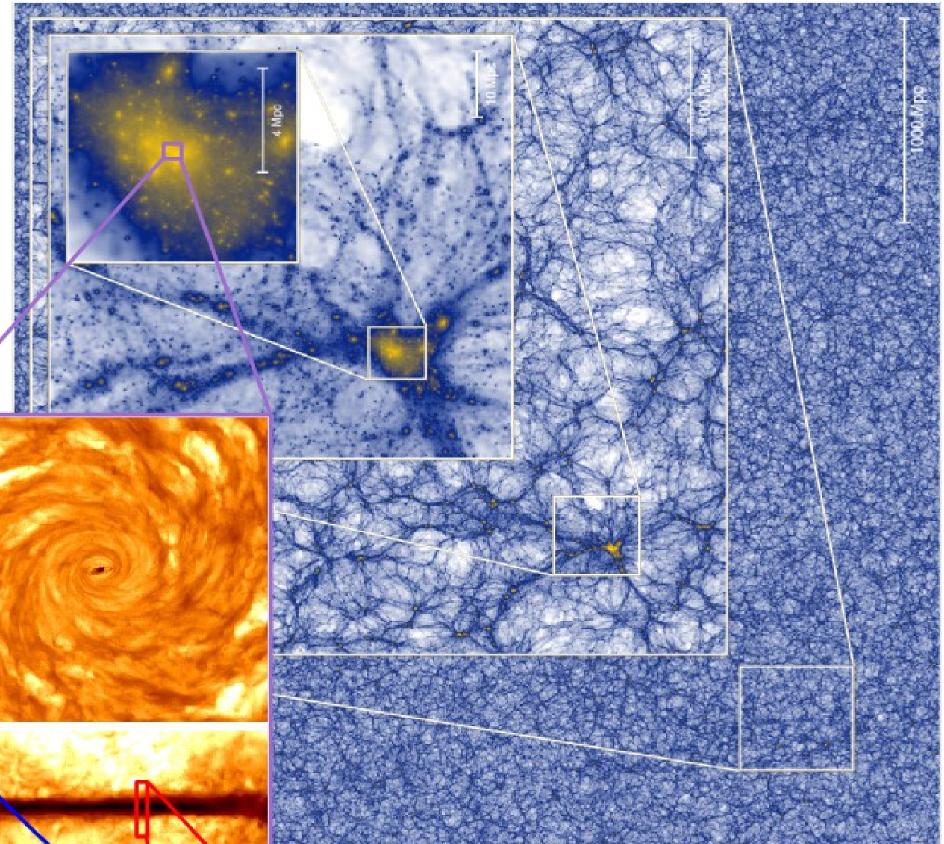

Angulo et al. (2012)

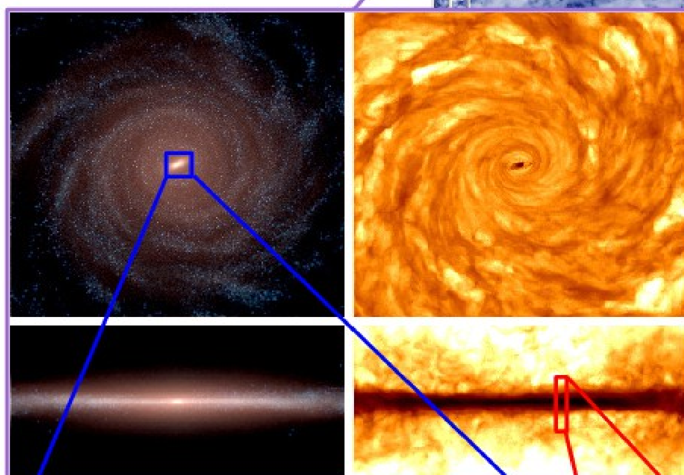

Grand et al. (2016)

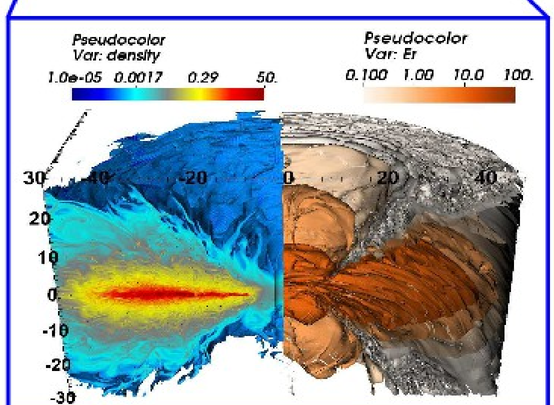

Jiang, Stone & Davis (2014)

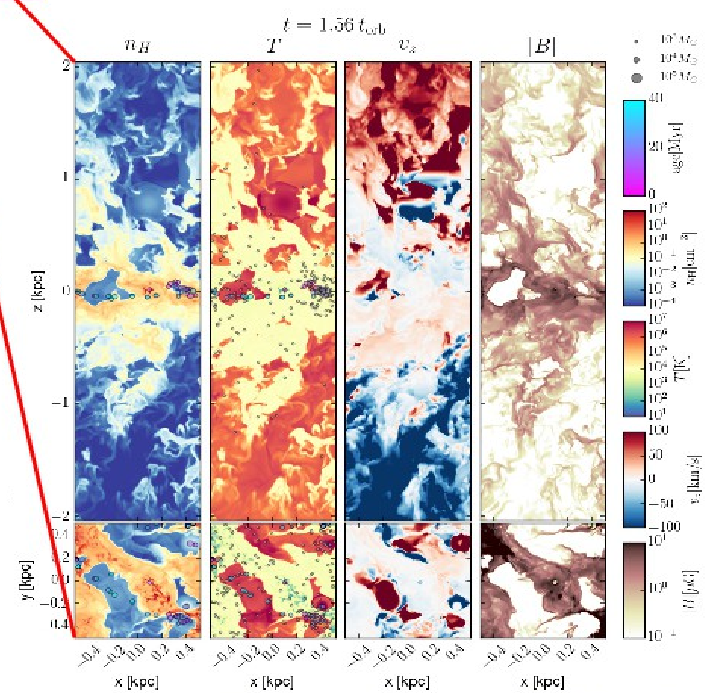

Kim & Ostriker (2016)

The Illustris and **IllustrisTNG** cosmological simulations

Galaxy formation physics in the Illustris simulations

Cooling and metal enrichment

- Nine elements followed independently
- Mass and metal loss of stars treated continuously over time based on stellar population synthesis models (similar to Wirsma et al. 2009)
- Ionization balance and cooling from H and He followed with direct chemical network (Katz et al. 1996)
- Metal line cooling added through CLOUDY lookup tables in density, temperature and redshift
- Simple self-shielding correction (Rahmati et al. 2013)

Star formation and winds

- Variant of Springel & Hernquist (2003)
- Cold dense gas stabilized by an ISM equation of state
- Winds are phenomenologically introduced, with an energy given as a fixed fraction of the supernova energy
- The wind velocity is variable, the mass flux follows for energy-driven winds
- Fiducial model scales wind with local dark matter velocity dispersion
- Winds are launched outside of star-forming gas, and metal-loading can be reduced if desired

Black hole accretion and feedback

- Black hole seeding and accretion model (Springel et al. 2005)
- Quasar-mode feedback for high accretion rates
- Radio-mode feedback for low accretion rates based on bubble-heating model (Sijacki et al. 2006)
- Radiative AGN feedback (change in heating/cooling due to variation of UVB) in proximity to an active black hole
- Reduction of accretion rate in low-pressure/low-density regimes to avoid large hot bubbles around black holes in quiescent state
- Black holes tied to potential minimum of halos

Vogelsberger et al. (2013)

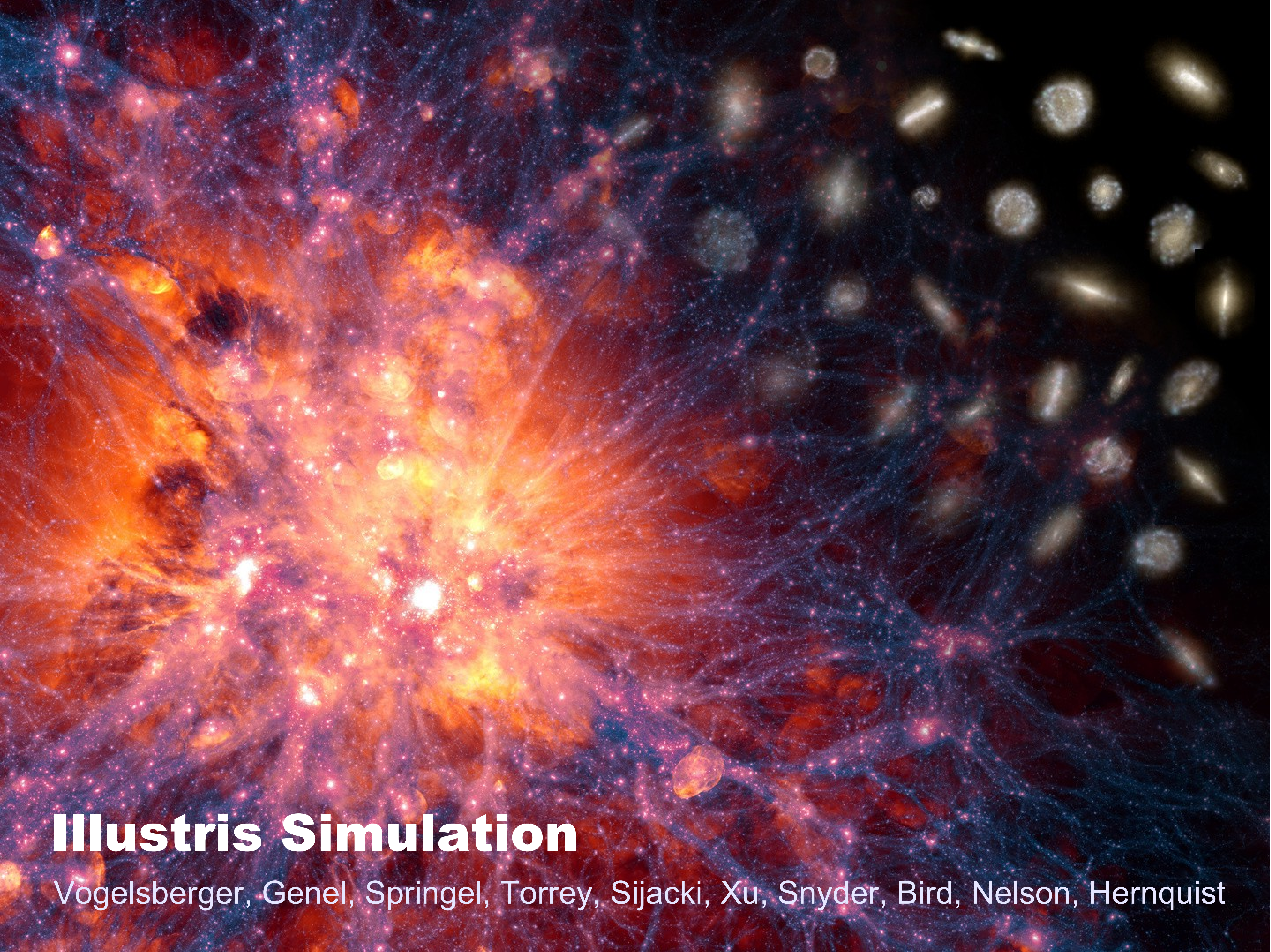
Illustris Simulation
Vogelsberger, Genel, Springel, Torrey, Sijacki, Xu, Snyder, Bird, Nelson, Hernquist

The Illustris simulation reproduces the morphological mix of galaxies

SIMULATED HUBBLE TUNING FORK DIAGRAM

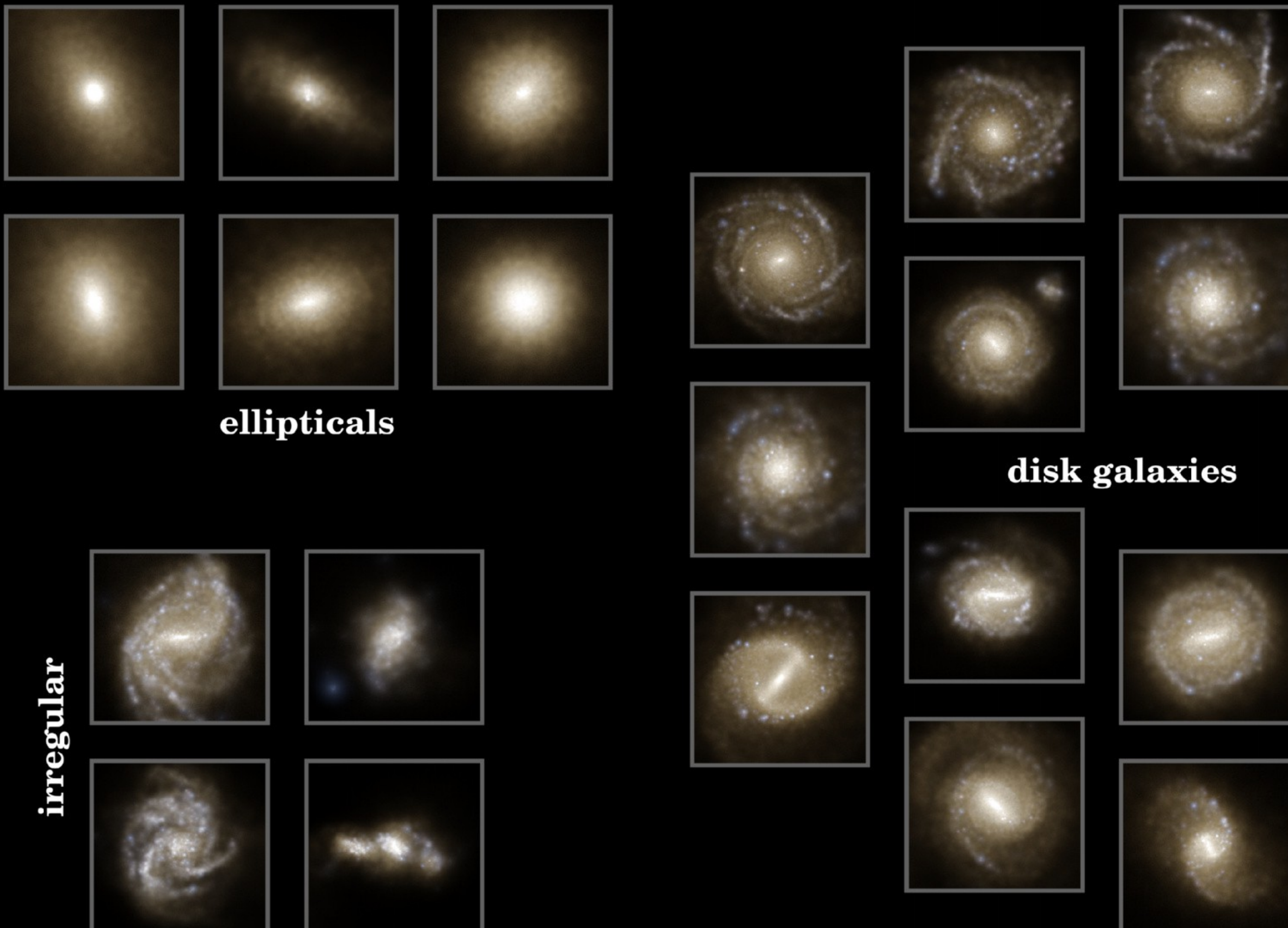

The stellar mass functions match observations at high redshift well

STELLAR MASS FUNCTIONS OF ILLUSTRIS COMPARED TO OBSERVATIONS AT DIFFERENT EPOCHS

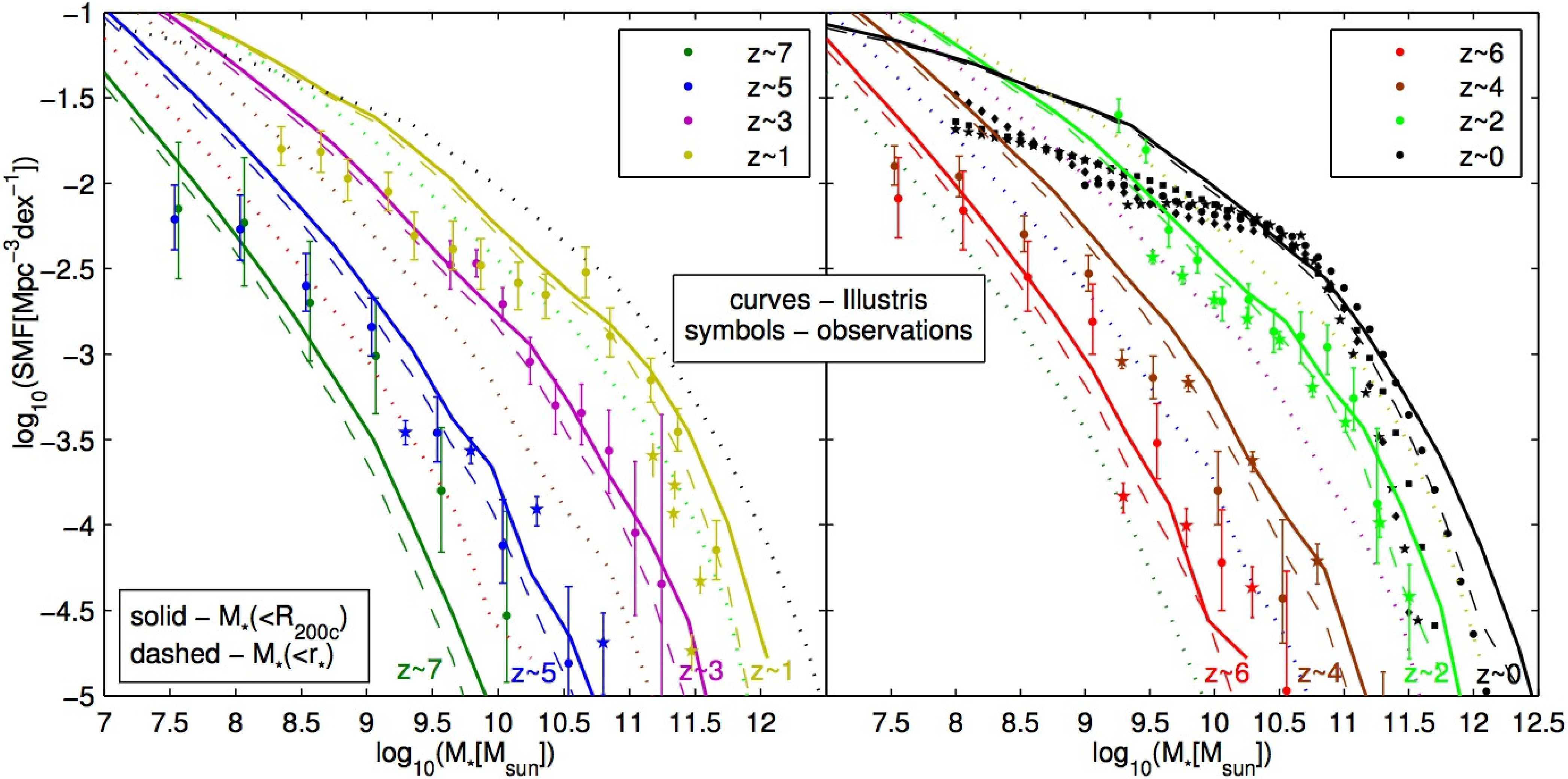

Genel et al. (2014)

People in the "Next Generation Illustris Simulations" team

A COLLABORATION BETWEEN HEIDELBERG, HARVARD, AND THE MIT

Volker Springel

Heidelberg Institute for Theoretical Studies
PI: Overall TNG Project

Lars Hernquist

Harvard University

Annalisa Pillepich

Max Planck Institute for Astronomy, Heidelberg
Co-PI: TNG50 Project

Rüdiger Pakmor

Heidelberg Institute for Theoretical Studies

Dylan Nelson

Max Planck Institute for Astrophysics, Garching
Co-PI: TNG50 Project

Rainer Weinberger

Heidelberg Institute for Theoretical Studies

Federico Marinacci

Massachusetts Institute of Technology

Jill Naiman

Harvard University

Mark Vogelsberger

Massachusetts Institute of Technology

Shy Genel

Center for Computational Astrophysics, Flatiron Institute

Paul Torrey

Massachusetts Institute of Technology

Jet injection by BHs can be modelled at high-resolution in individual "zoom" galaxy cluster simulations

HEATING CLUSTERS THROUGH JET-ICM INTERACTIONS

Weinberger et al. (2017)

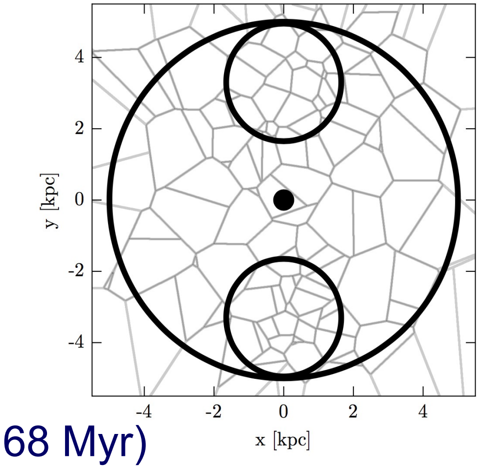

Jet after 42 Myr

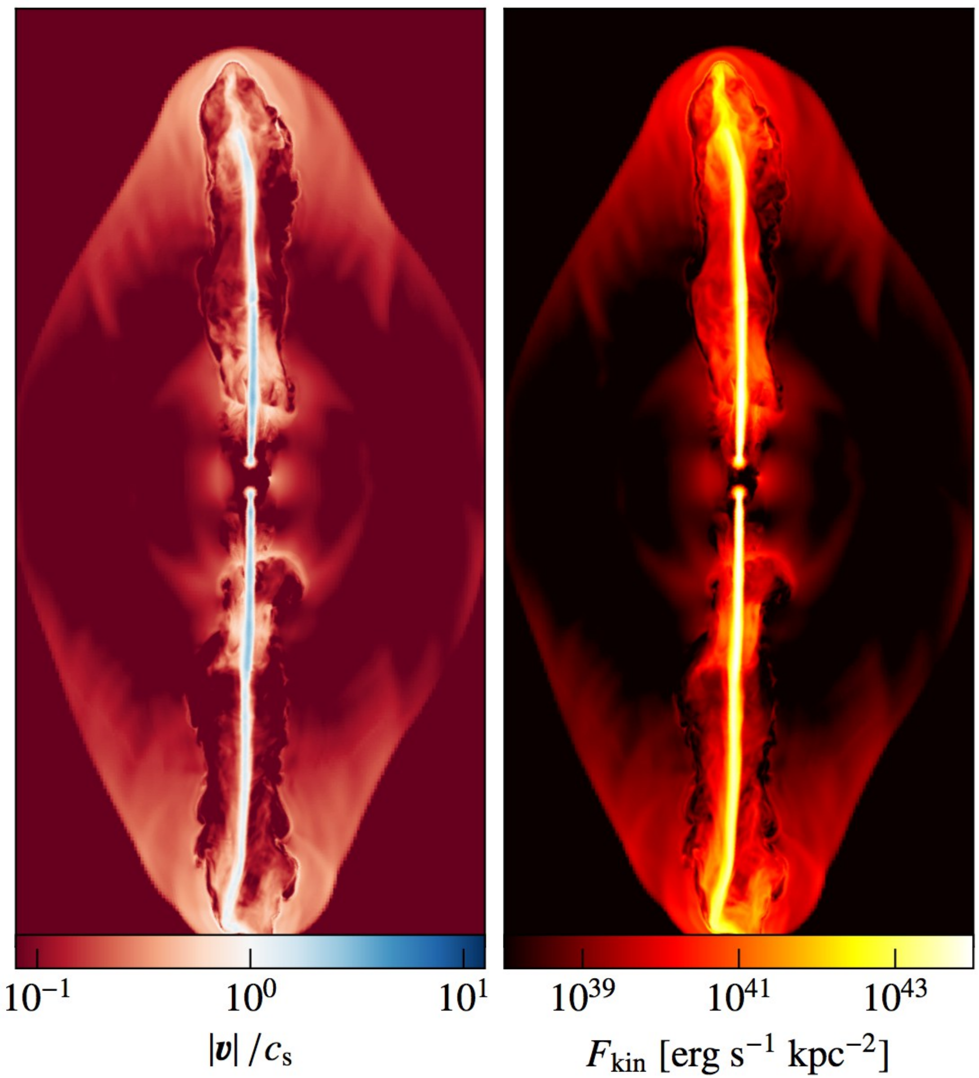

ICM after lobe passage (168 Myr)

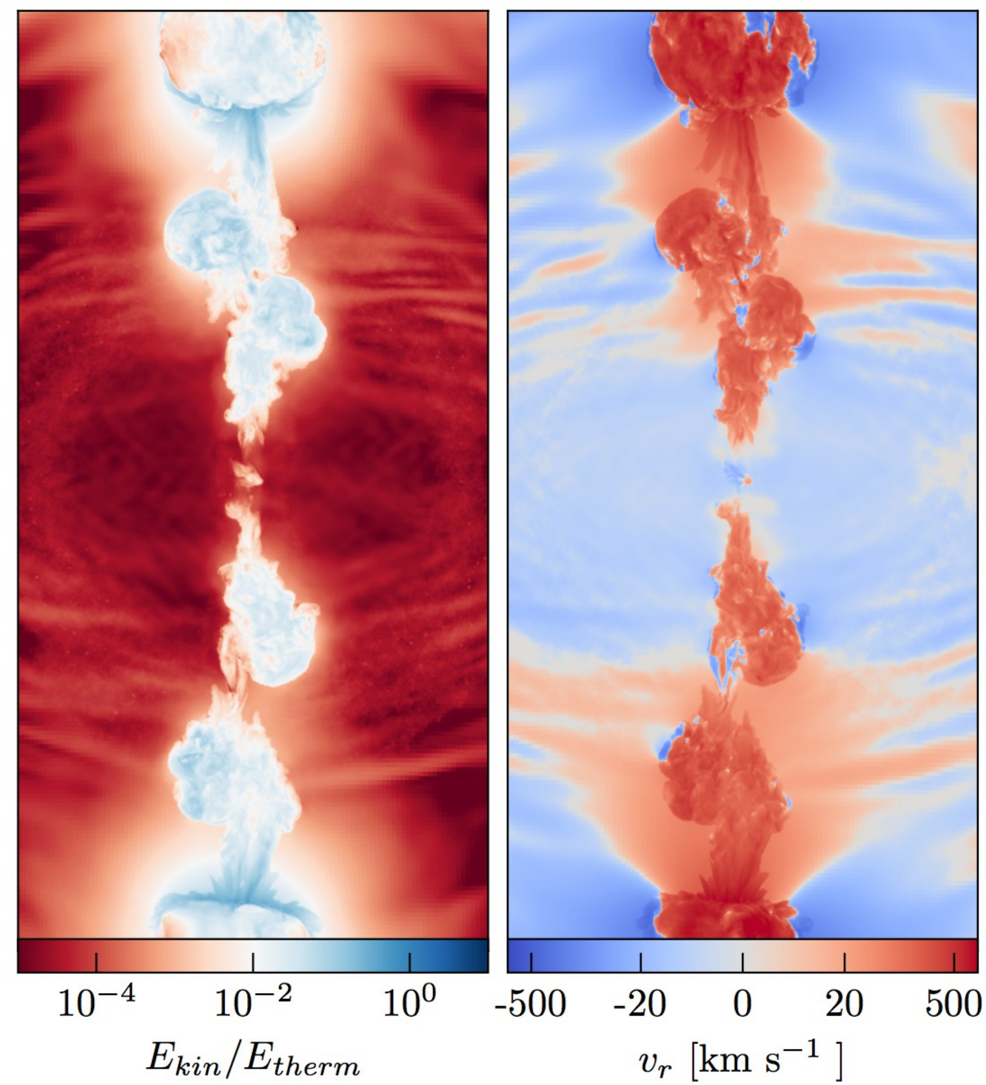

Intense winds from supermassive black holes may keep ‘red geyser’ galaxies turned off

EXAMPLE OF OBSERVATIONAL EVIDENCE FOR BLACK HOLE WINDS

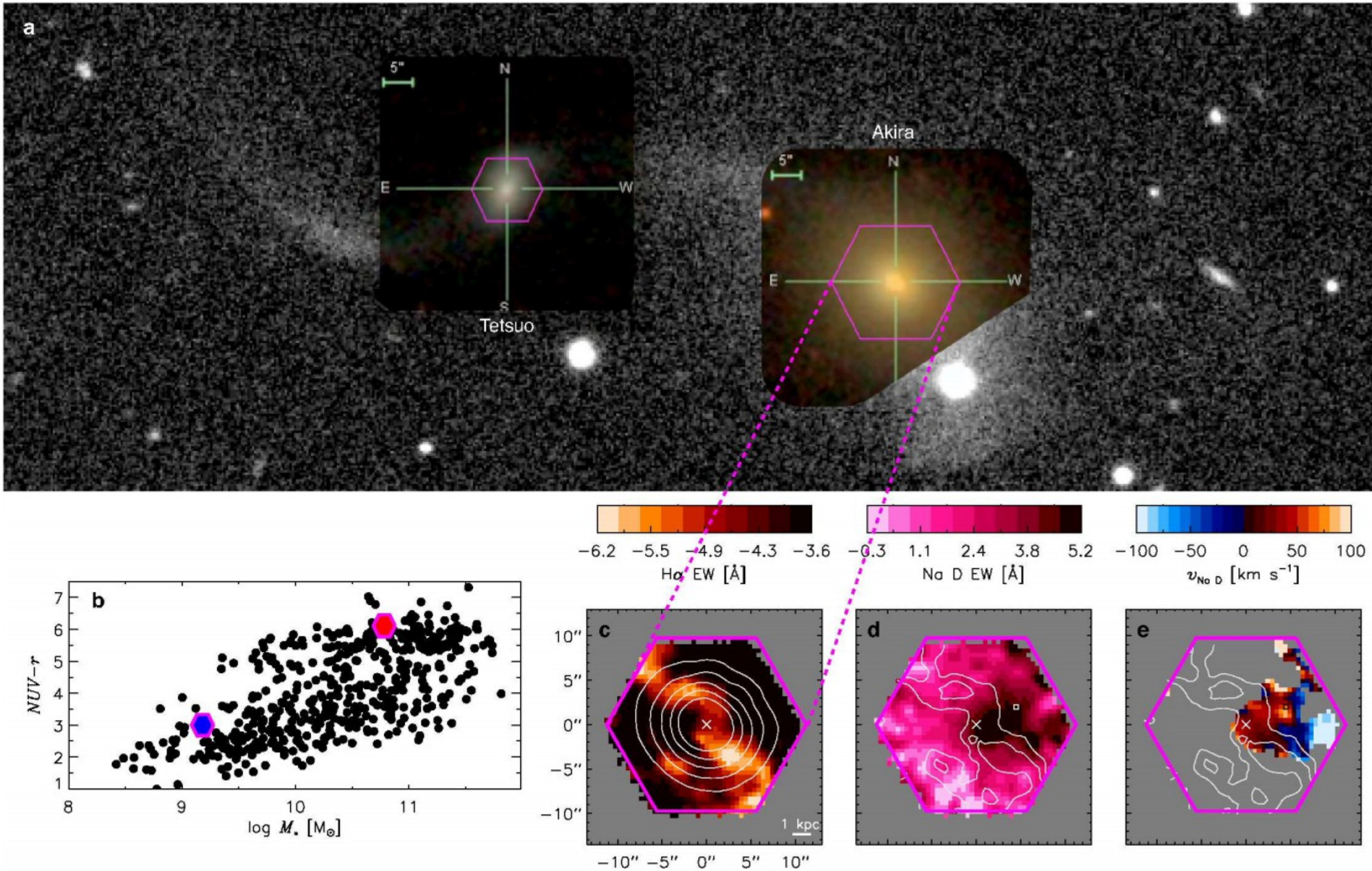

Cheung et al. (2016, Nature, 533, 504)

(Genzel et al. 2014, Förster Schreiber et al. 2014)

We have adopted a simple model for kinetic AGN winds in cosmological simulations of galaxy formation

ILLUSTRIS-TNG AGN MODEL AND ITS IMPACT

$$\dot{M}_{\rm Bondi} = \frac{4\pi G^2 M_{\rm BH}^2 \rho}{c_s^3}$$

$$\dot{M}_{\rm Edd} = \frac{4\pi G M_{\rm BH} m_p}{\epsilon_r \sigma_T c}$$

We distinguish a "high" and a "low" accretion flow state:

$$\frac{\dot{M}_{\rm Bondi}}{\dot{M}_{\rm Edd}} \geq \chi = \min\left[\chi_0 \left(\frac{M_{\rm BH}}{10^8\,{\rm M}_\odot}\right)^\beta, 0.1\right]$$

Pure thermal feedback in "high" quasar mode:

$$\Delta \dot{E}_{\rm high} = \epsilon_{\rm f,high} \epsilon_{\rm r} \dot{M}_{\rm BH}\, c^2$$

Pure kinetic feedback in "low" radio mode:

$$\Delta \dot{E}_{\rm low} = \epsilon_{\rm f,kin} \dot{M}_{\rm BH} c^2.$$

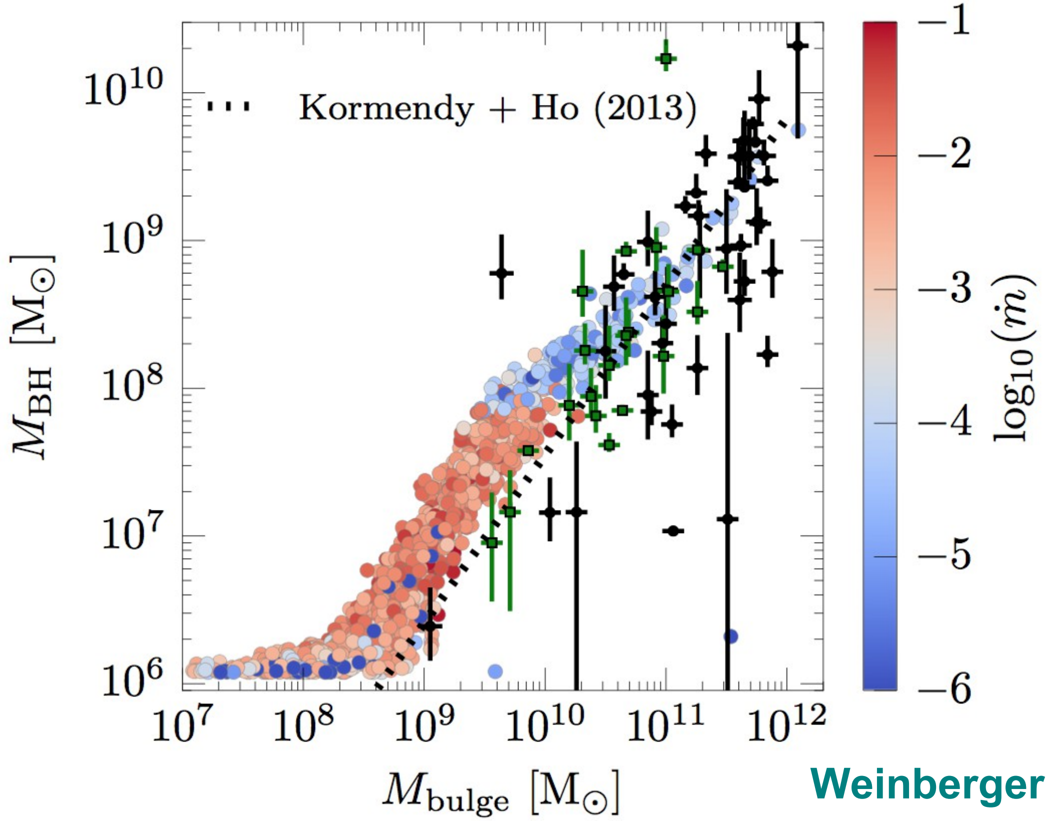

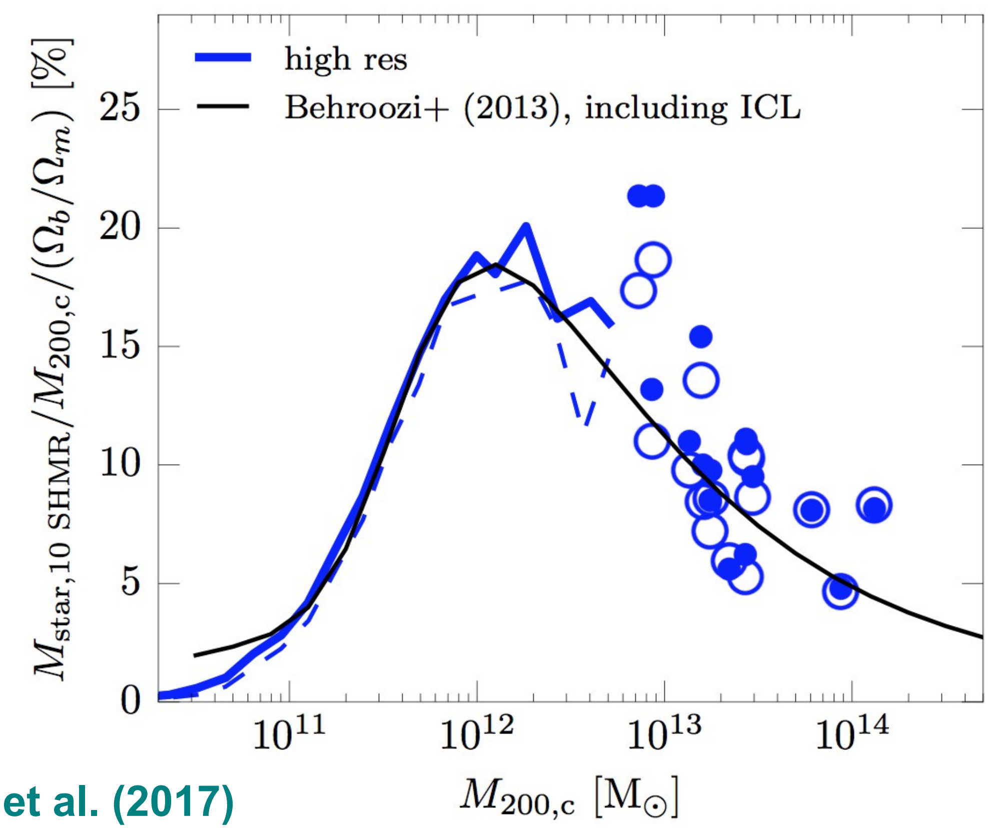

Weinberger et al. (2017)

We obtain **sudden** quenching, setting in at around $M_* \sim 2 \times 10^{10}$ $M_{\rm sun}$

The gas fractions in galaxy groups and poor clusters provide a sensitive constraint on viable AGN feedback models

GAS FRACTIONS WITH THE NEW ILLUSTRIS-TNG AGN MODEL

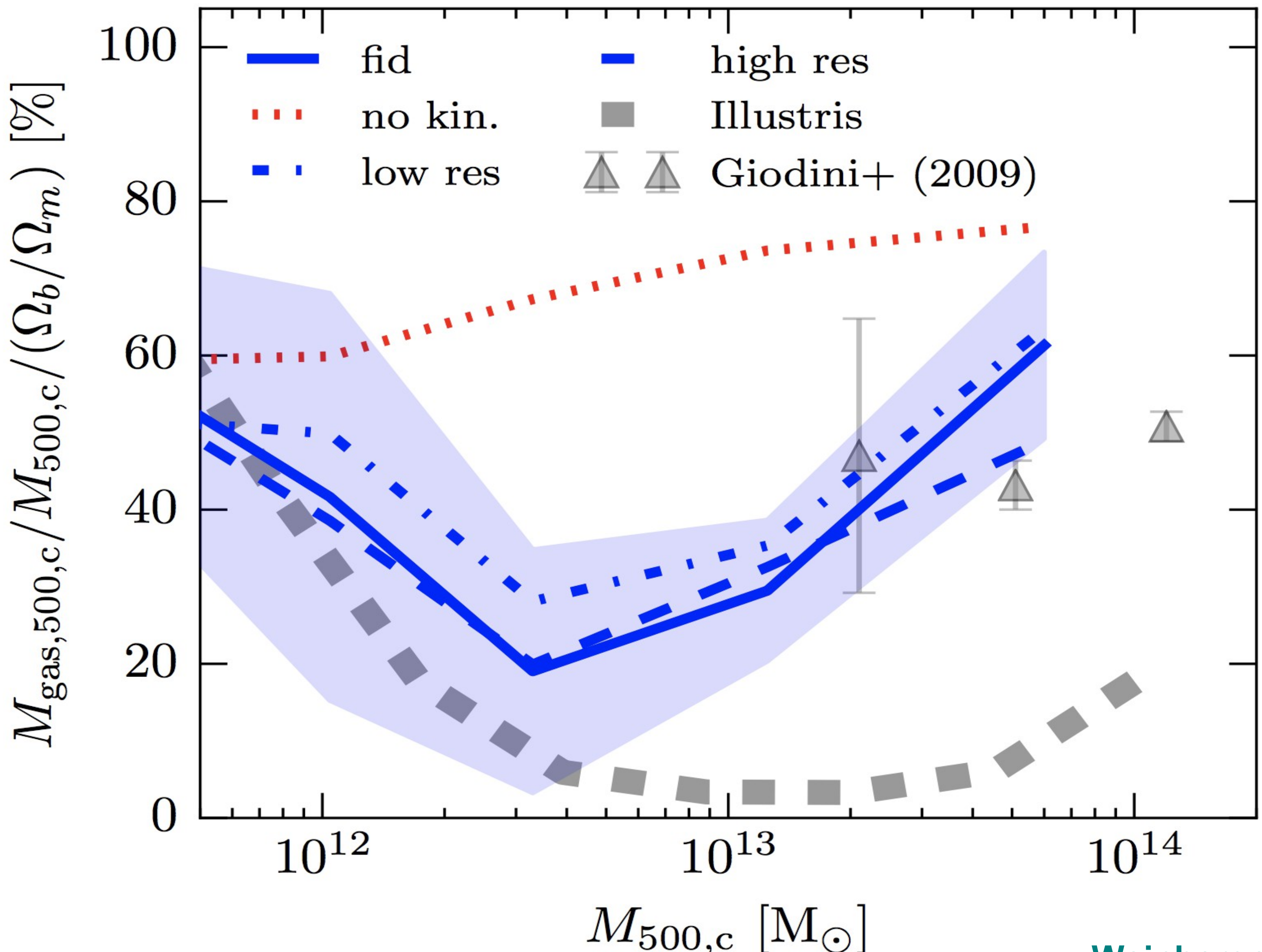

Weinberger et al. (2017)

The “Next Generation Illustris Simulations” (IllustrisTNG) are our novel, significantly improved models for cosmic structure formation

DIFFERENT SIMULATIONS OF THE ILLUSTRIS-TNG PROJECT

IllustrisTNG Collaboration (2017)

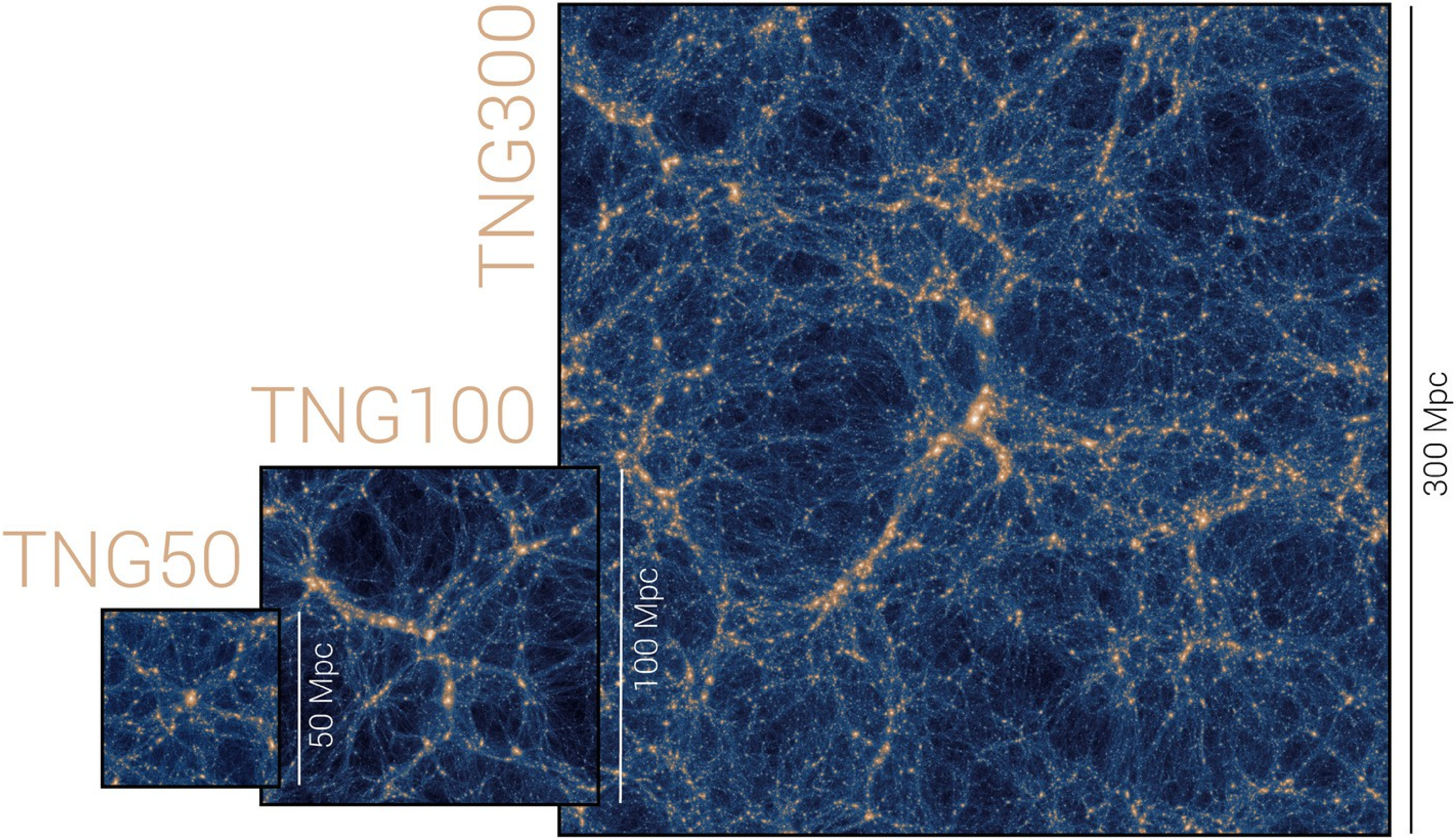

Overview over the simulation set of IllustrisTNG

RUNS WERE DONE ON HAZEL-HEN AT HLRS WITH CPU-TIME GRANTED BY GCS

Series	Run	Boxsize $[h^{-1}\mathrm{Mpc}]$	Boxsize $[\mathrm{Mpc}]$	N_{gas}	N_{dm}	N_{tracer}	m_{b} $[h^{-1}\mathrm{M}_\odot]$	m_{dm} $[h^{-1}\mathrm{M}_\odot]$	ϵ $[h^{-1}\mathrm{kpc}]$
TNG300	TNG300(-1)	205	302.6	2500^3	2500^3	2500^3	7.44×10^6	3.98×10^7	1.0
up to	TNG300-2	205	302.6	1250^3	1250^3	1250^3	5.95×10^7	3.19×10^8	2.0
24000	TNG300-3	205	302.6	625^3	625^3	625^3	4.76×10^8	2.55×10^9	4.0
cores,	TNG300-DM(-1)	205	302.6		2500^3			4.73×10^7	1.0
35 Mio	TNG300-DM-2	205	302.6		1250^3			3.78×10^8	2.0
core-h	TNG300-DM-3	205	302.6		625^3			3.03×10^9	4.0
TNG100	TNG100(-1)	75	110.7	1820^3	1820^3	2×1820^3	9.44×10^5	5.06×10^6	0.5
up to	TNG100-2	75	110.7	910^3	910^3	2×910^3	7.55×10^6	4.04×10^7	1.0
10720	TNG100-3	75	110.7	455^3	455^3	2×455^3	6.04×10^7	3.24×10^8	2.0
cores,	TNG100-DM(-1)	75	110.7		1820^3			6.00×10^6	0.5
18 Mio	TNG100-DM-2	75	110.7		910^3			4.80×10^7	1.0
core-h	TNG100-DM-3	75	110.7		455^3			3.84×10^8	2.0
TNG50	TNG50-1	35	51.7	2160^3	2160^3	2160^3	5.74×10^4	3.07×10^5	0.2
	TNG50-2	35	51.7	1080^3	1080^3	1080^3	4.59×10^5	2.46×10^6	0.4
up to	TNG50-3	35	51.7	540^3	540^3	540^3	3.67×10^6	1.97×10^7	0.8
24000	TNG50-4	35	51.7	270^3	270^3	270^3	2.94×10^7	1.57×10^8	1.6
cores,	TNG50-DM-1	35	51.7		2160^3			3.64×10^5	0.2
90 Mio	TNG50-DM-2	35	51.7		1080^3			2.92×10^6	0.4
core-h	TNG50-DM-3	35	51.7		540^3			2.33×10^7	0.8
	TNG50-DM-4	35	51.7		270^3			1.87×10^8	1.6

IllustrisTNG was executed on **Hazel Hen** in Stuttgart, Germany

GCS
Gauss Centre for Supercomputing

7.4 PFlops

IllustrisTNG gives detailed predictions for the spatial distribution of stars, and its relation to the underlying dark matter backbone

DARK MATTER AND STELLAR DENSITY IN ILLUSTRIS-TNG

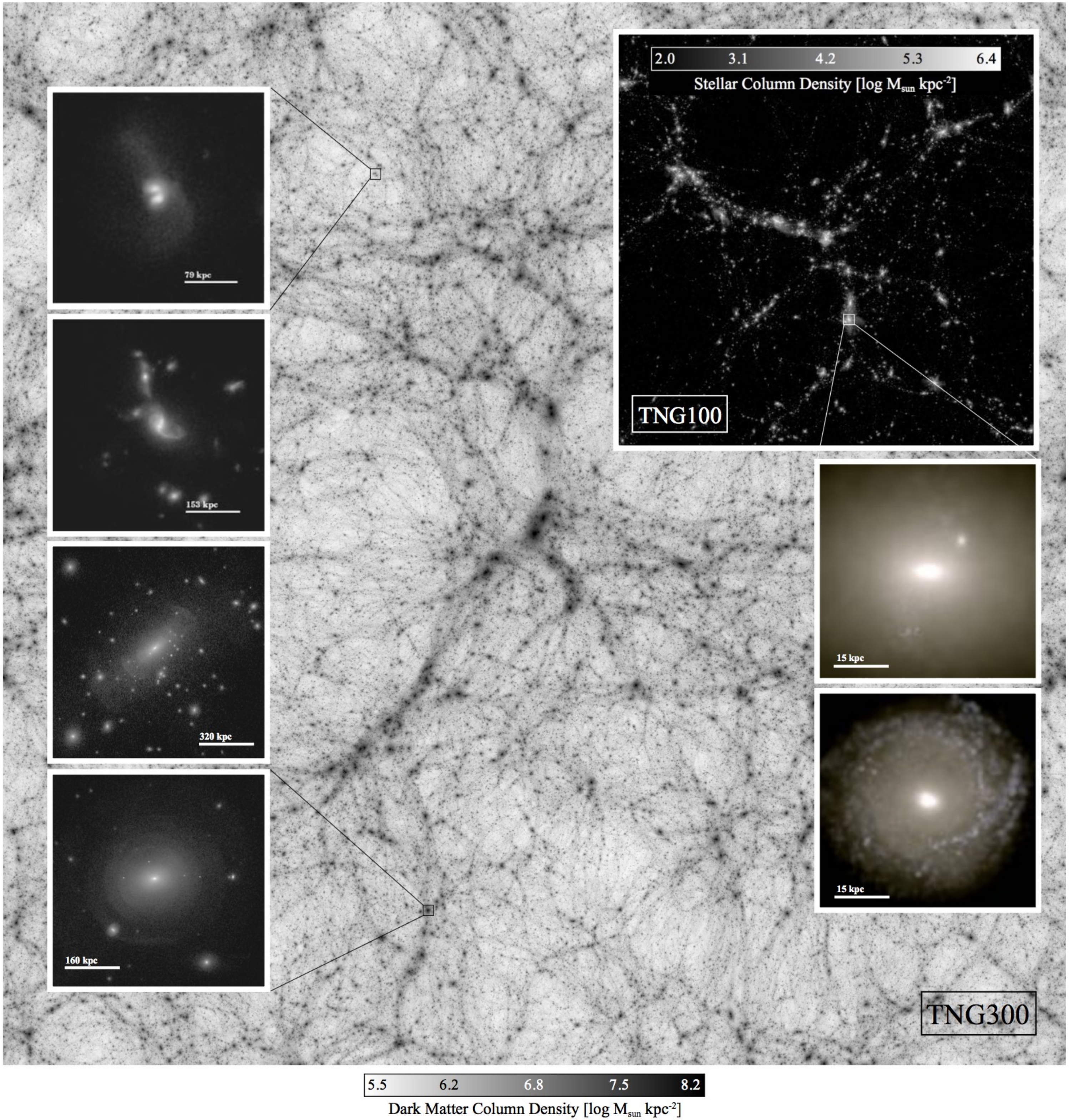

Pillepich et al. (2018)

IllustrisTNG reproduces the observed color-bimodality of galaxies thanks to AGN feedback

COLOR DISTRIBUTION OF GALAXIES OF DIFFERENT MASS COMPARED TO SDSS

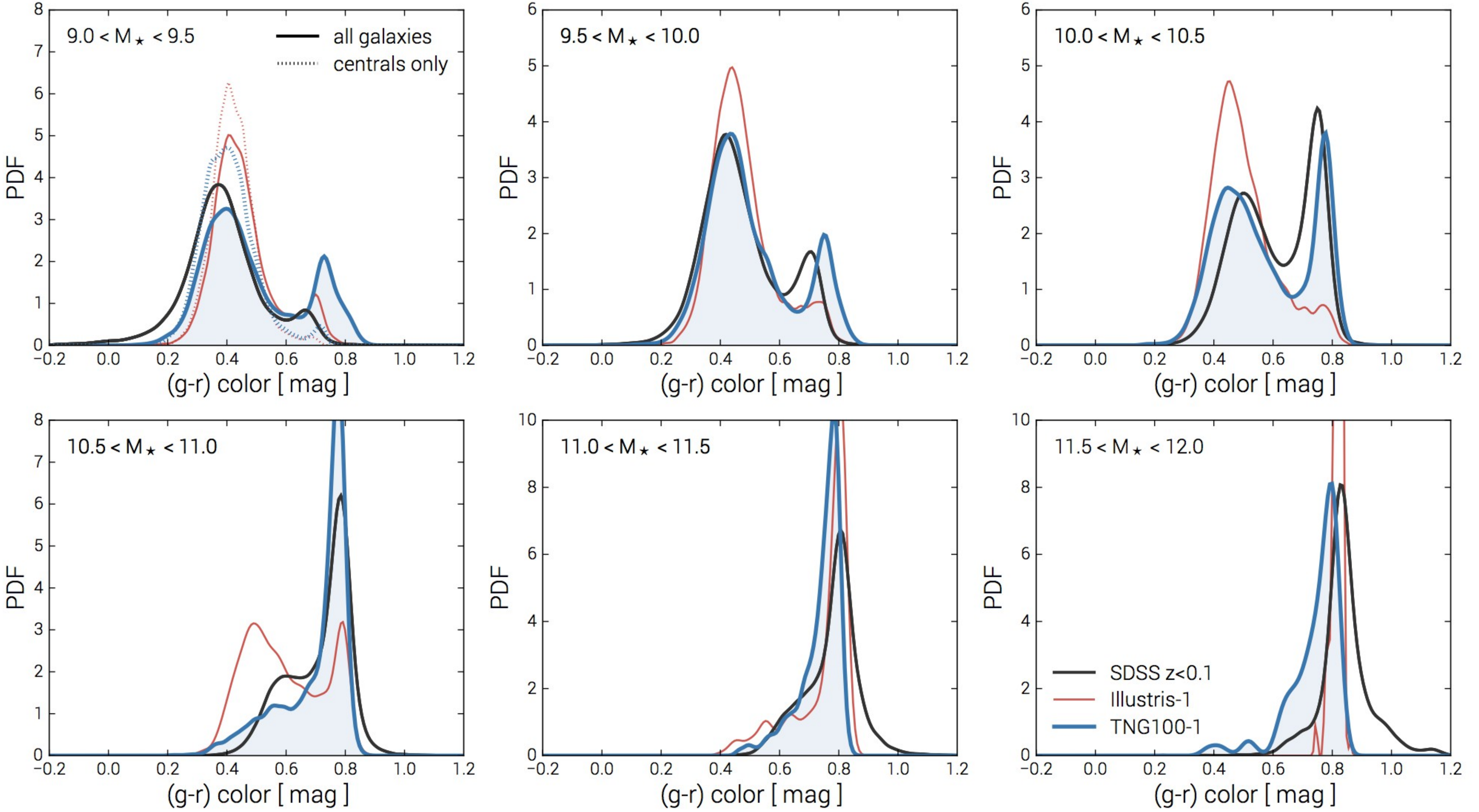

Nelson et al. (2017)

The new feedback model in TNG produces a sharp characteristic scale in the halo – stellar mass relationship

ILLUSTRIS COMPARED TO ABUNDANCE MATCHING MODELS FOR THE SMHM RELATION

Pillepich et al. (2018)

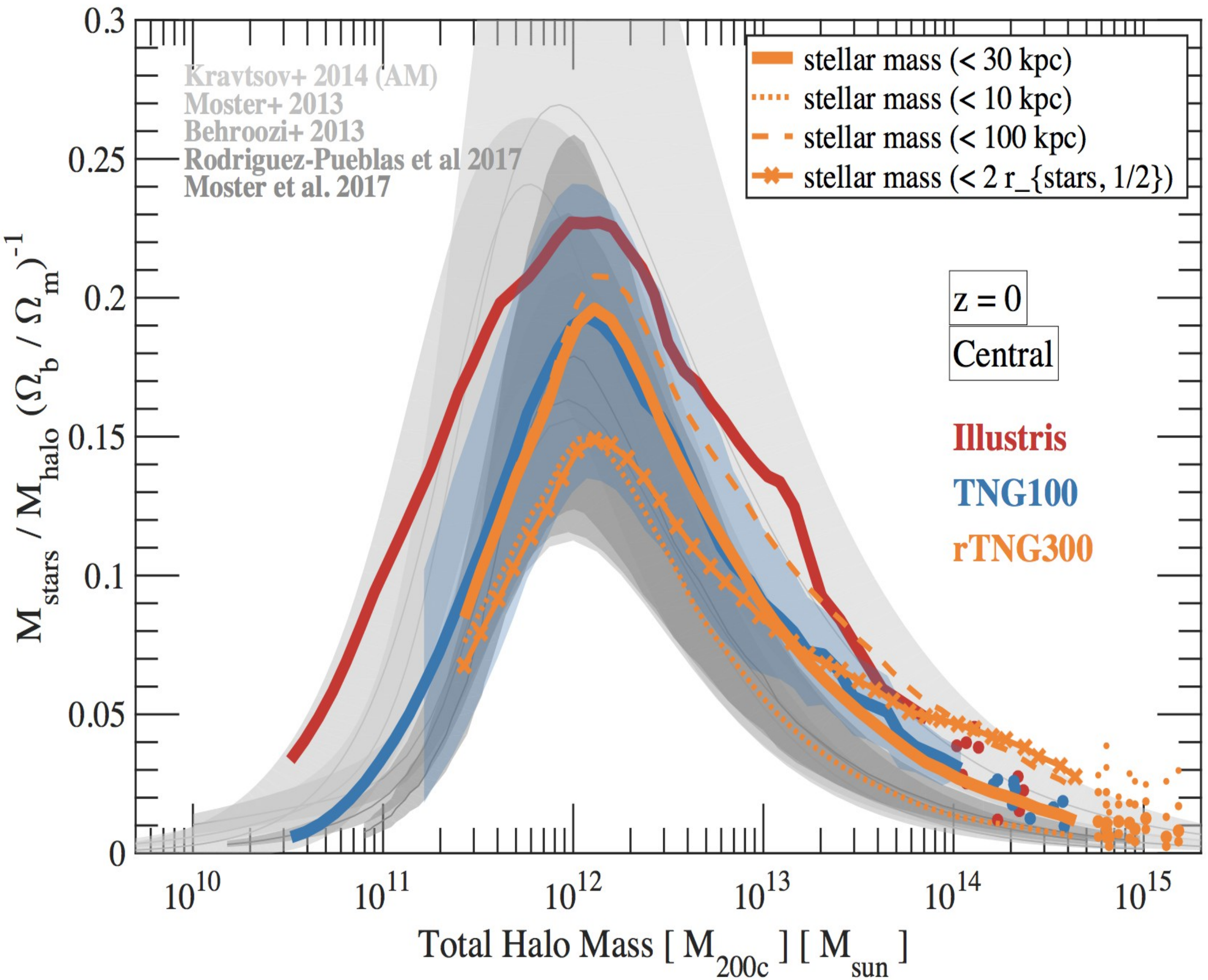

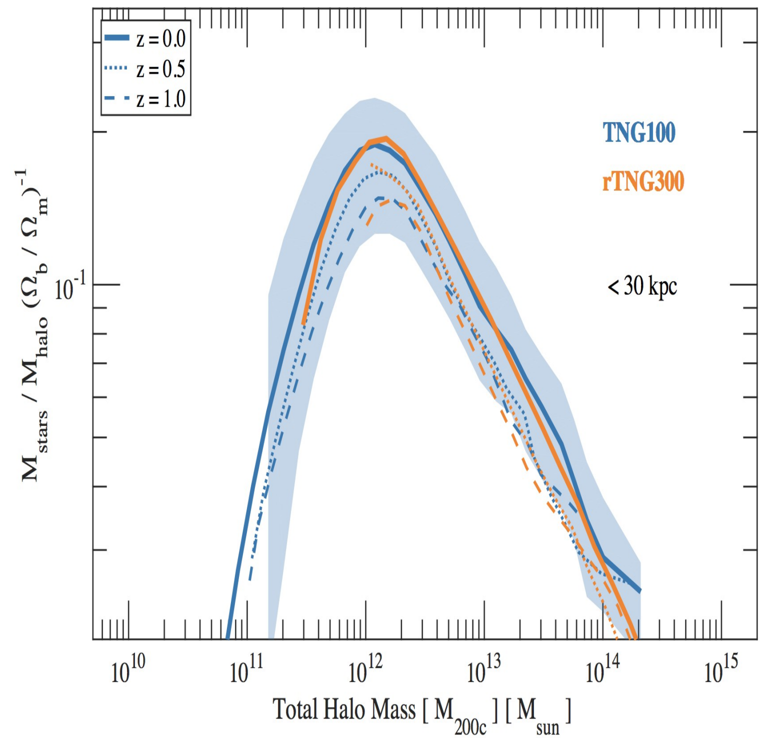

Kinetic AGN feedback takes over at late times in large galaxies

FEEDBACK ENERGY AS A FUNCTION OF TIME AND FINAL STELLAR MASS

Weinberger et al. (2018)

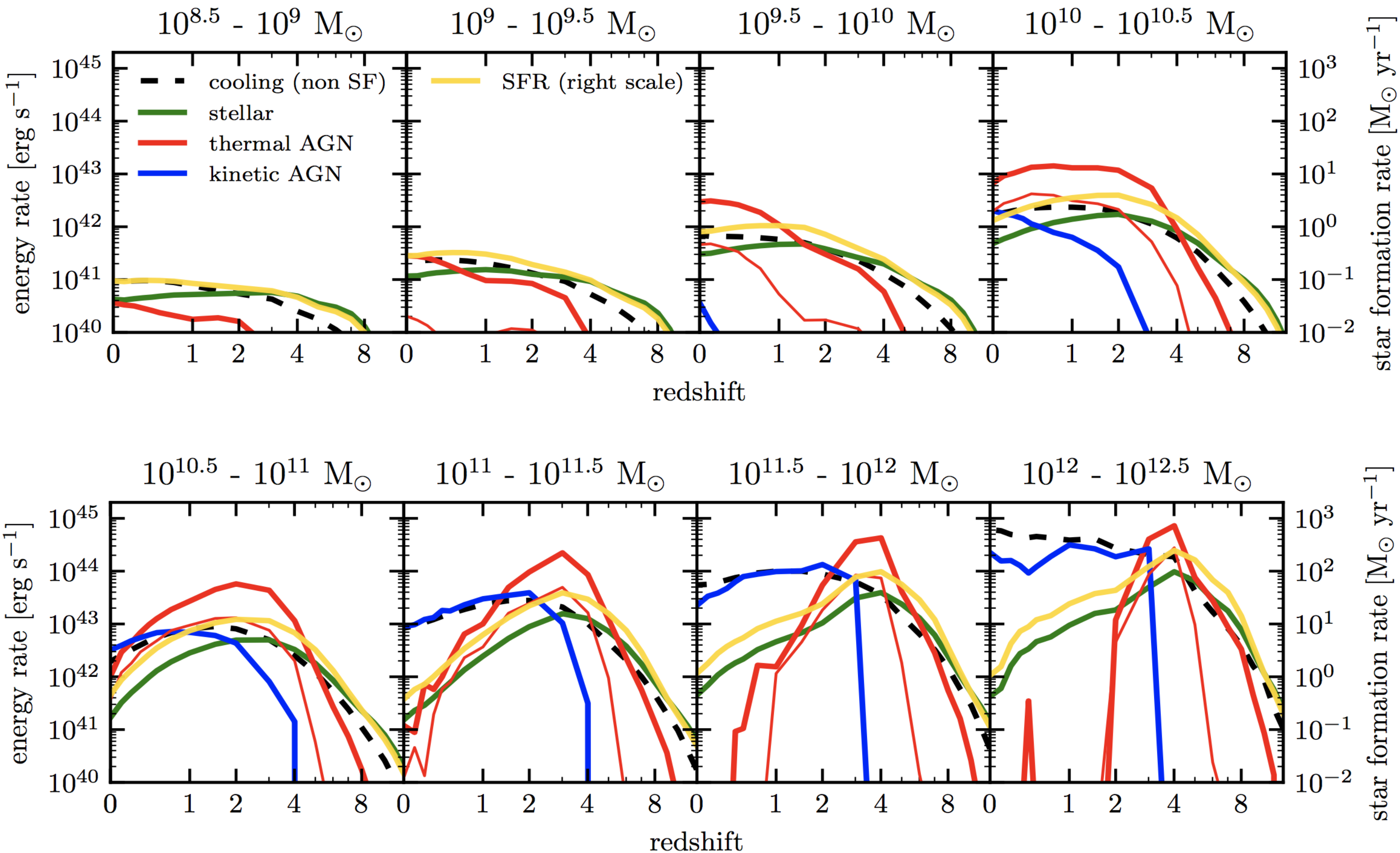

IllustrisTNG predicts galaxy correlation functions in good agreement with the most accurate galaxy surveys

PROJECTED TWO-POINT FUNCTIONS IN DIFFERENT MASS BINS

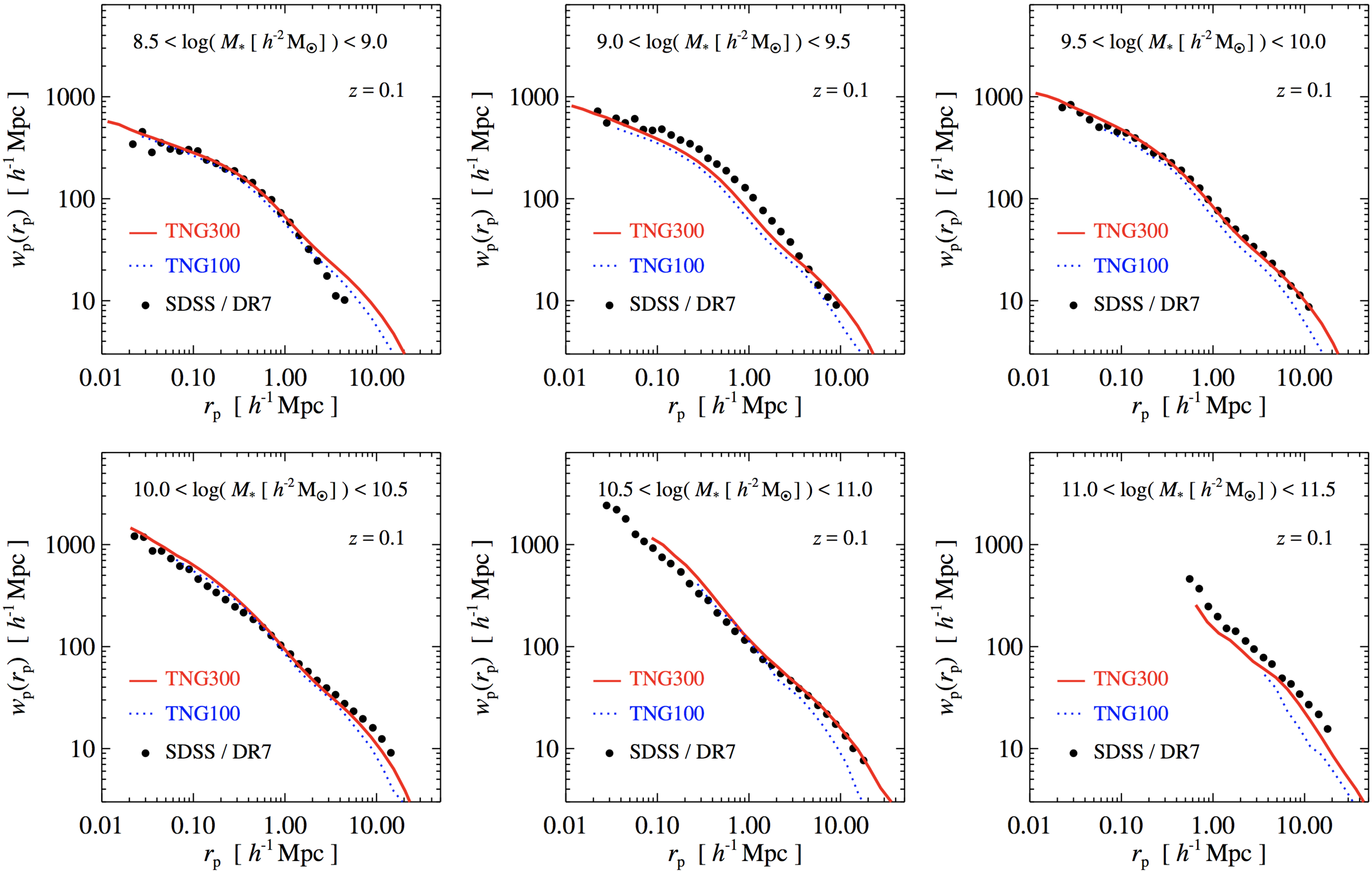

IllustrisTNG predicts pronounced differences in the clustering of red and blue galaxies in good agreement with data

CLUSTERING IN DIFFERENT MASS AND COLOR BINS COMPARED TO SDSS

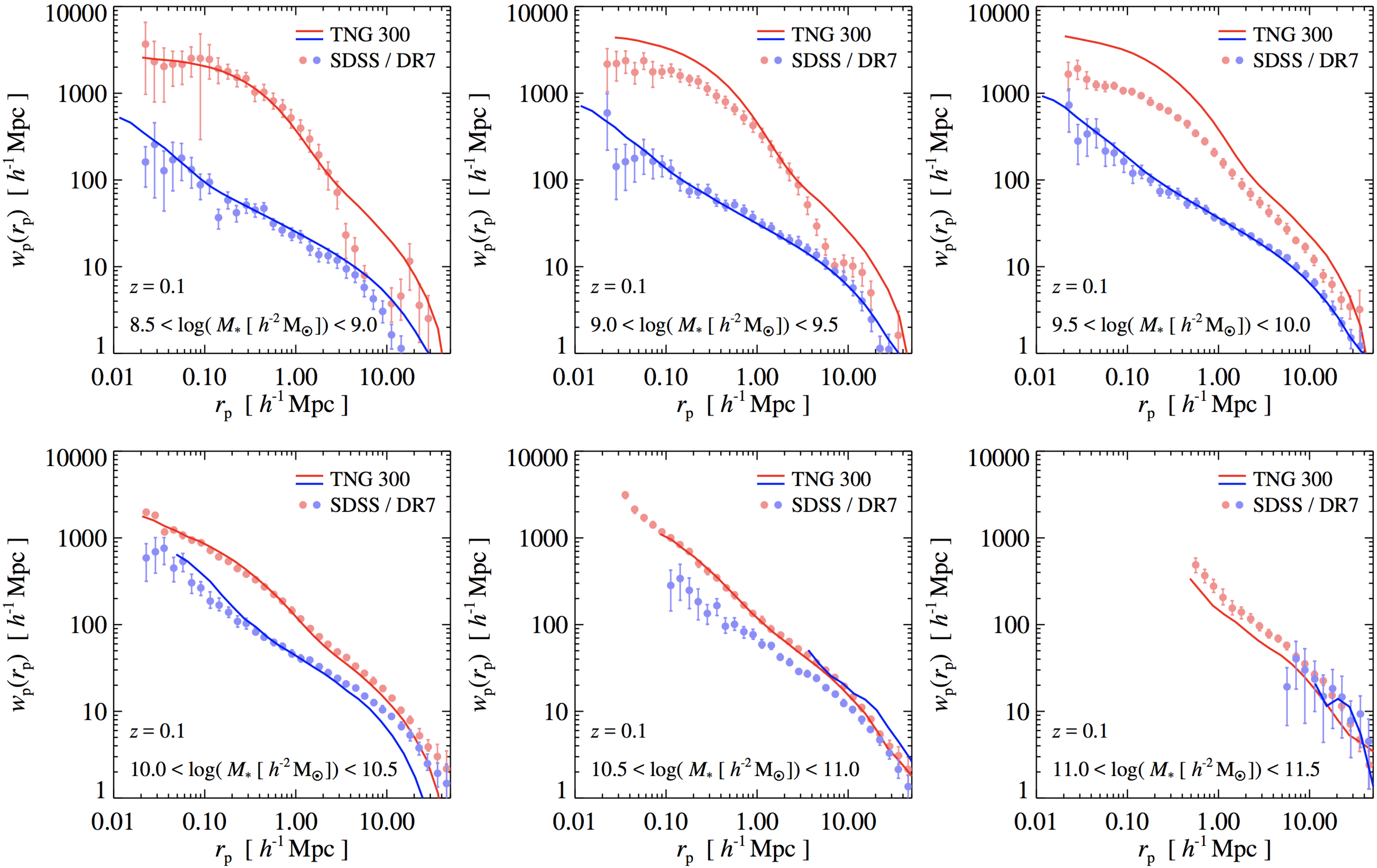

IllustrisTNG predicts that the correlation length of galaxy clustering depends both on stellar mass and redshift

CORRELATION LENGTH AS A FUNCTION OF REDSHIFT AND STELLAR MASS

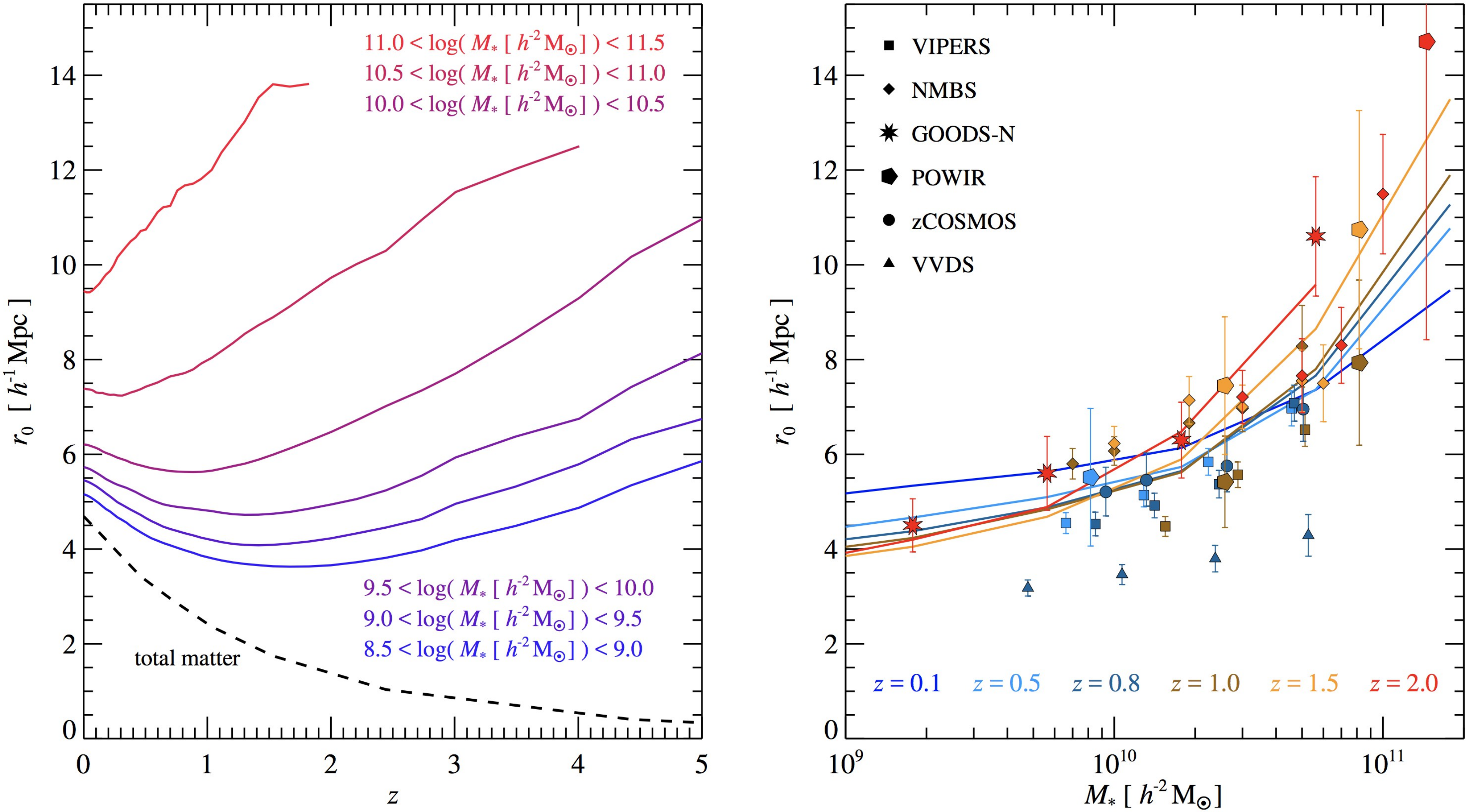

Baryonic affects on the matter power spectrum are at the 20% level on scales of k~10 h/Mpc

RELATIVE IMPACT ON POWER SPECTRUM AT DIFFERENT EPOCH AND IN DIFFERENT SIMULATIONS

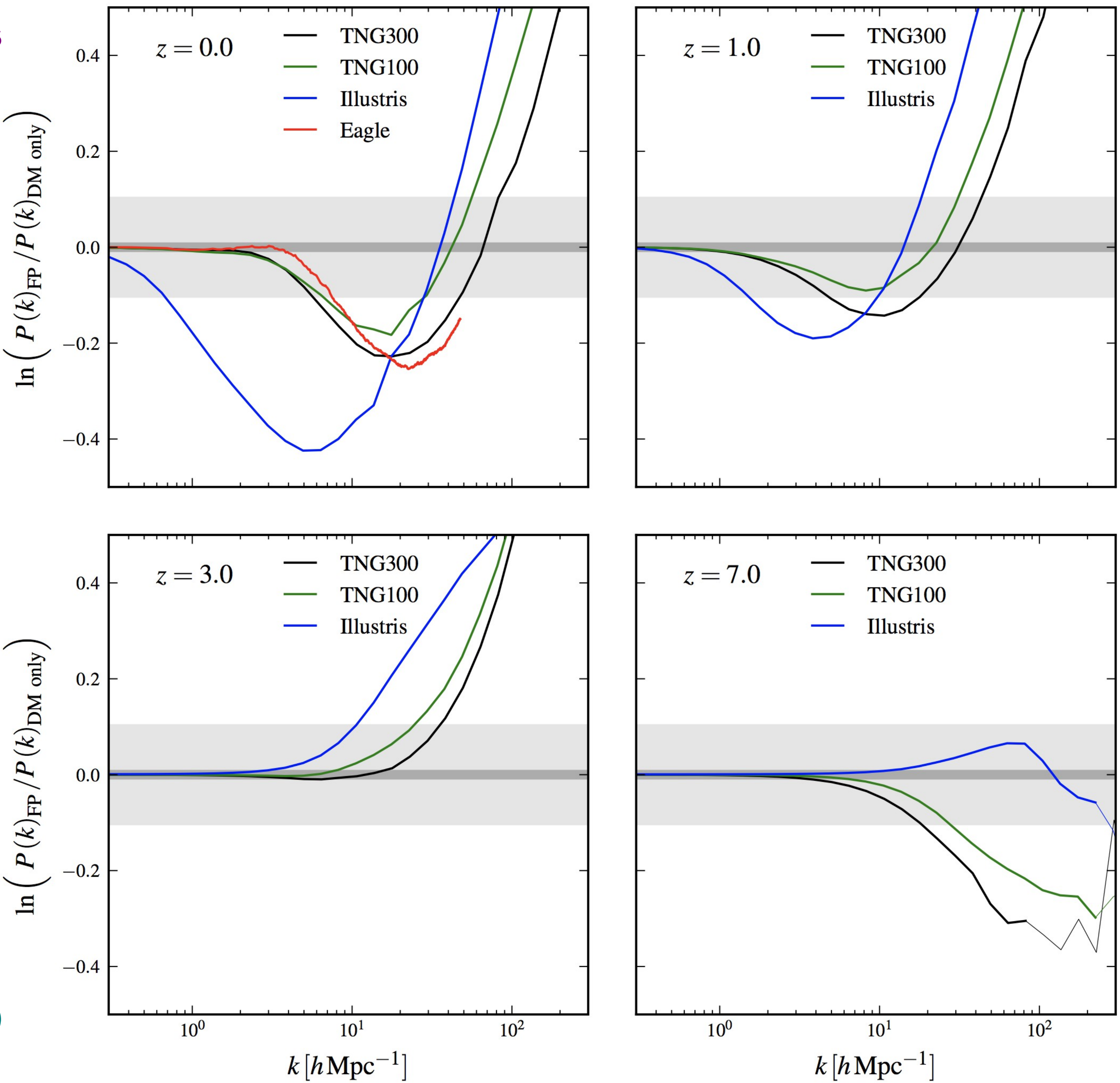

Springel et al. (2017)

TNG allows us to measure the scale-dependence of the power spectrum of different tracers relative to the non-linear clustering of all the matter

SCALE-DEPENDENT BIAS IN THE POWER SPECTRUM OF DIFFERENT TRACERS

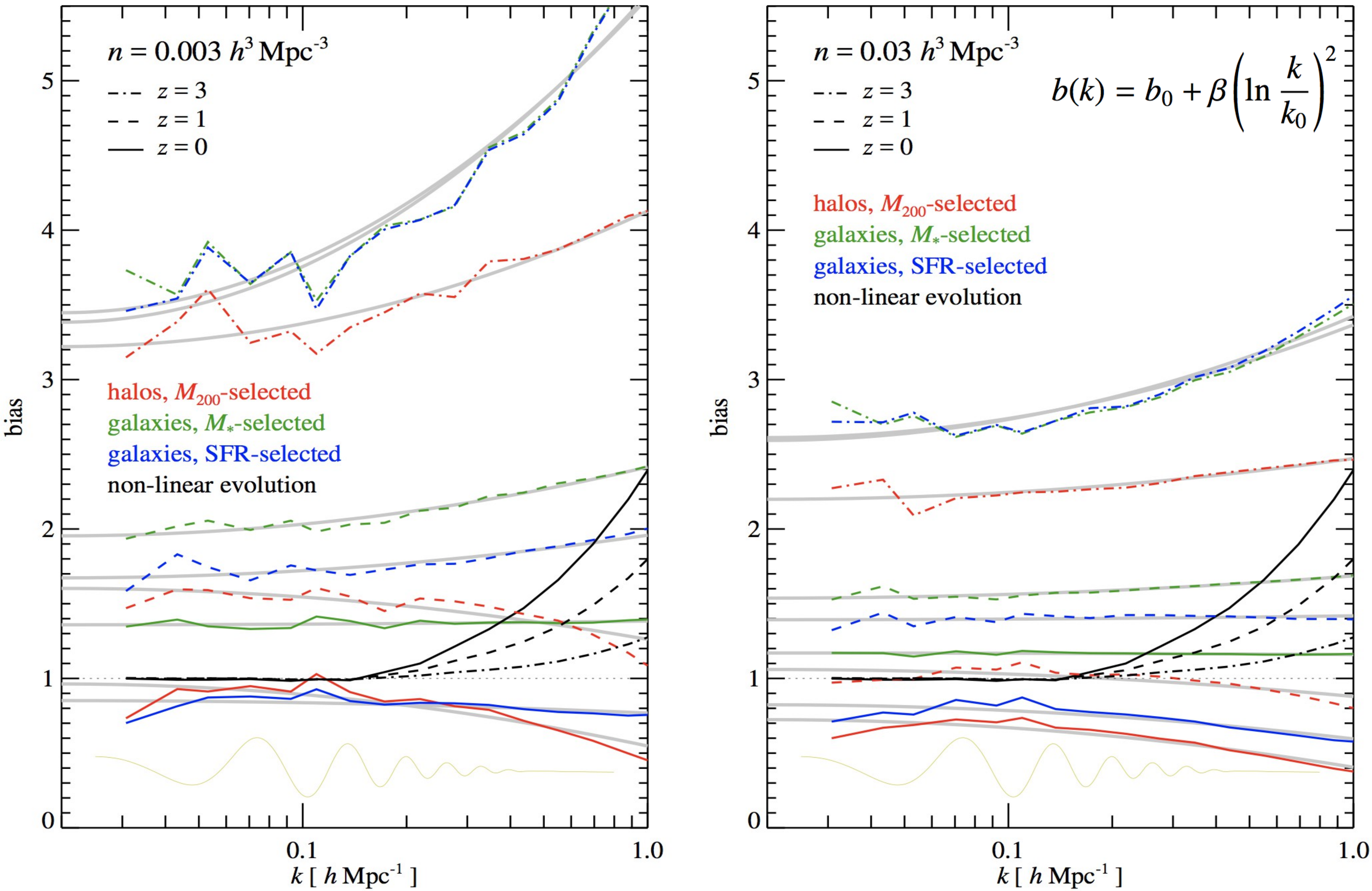

Scale-dependent bias can induce a nominal shift in the peak positions of BAOs

PREDICTED BAO SHAPE FOR DIFFERENT TRACERS

Shifts of ~5% in scale occur, but template fitting to (perfect) data can compensate for that, leaving one with residuals of order ~0.1%.

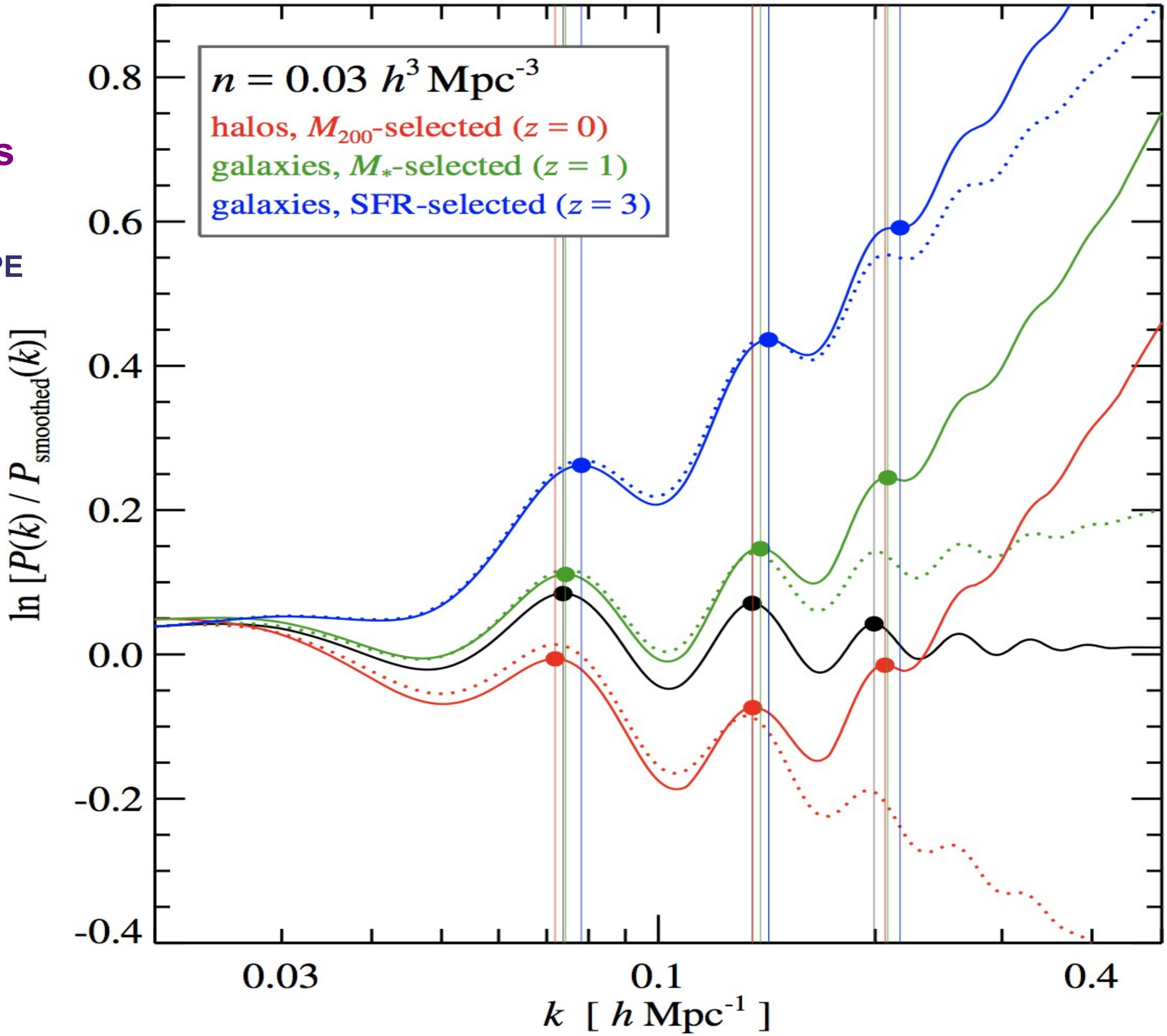

$$P_{\mathrm{obs}}(k) = (c_0 + c_1 k + c_2 k^2) P_{\mathrm{lin}}(k/\alpha)$$

Black hole growth influences disk sizes

BLACK HOLE GROWTH BETWEEN Z=1 AND Z=0 CORRELATES WITH DISK SCALE LENGTHS IN HALOS OF MILKY WAY MASS

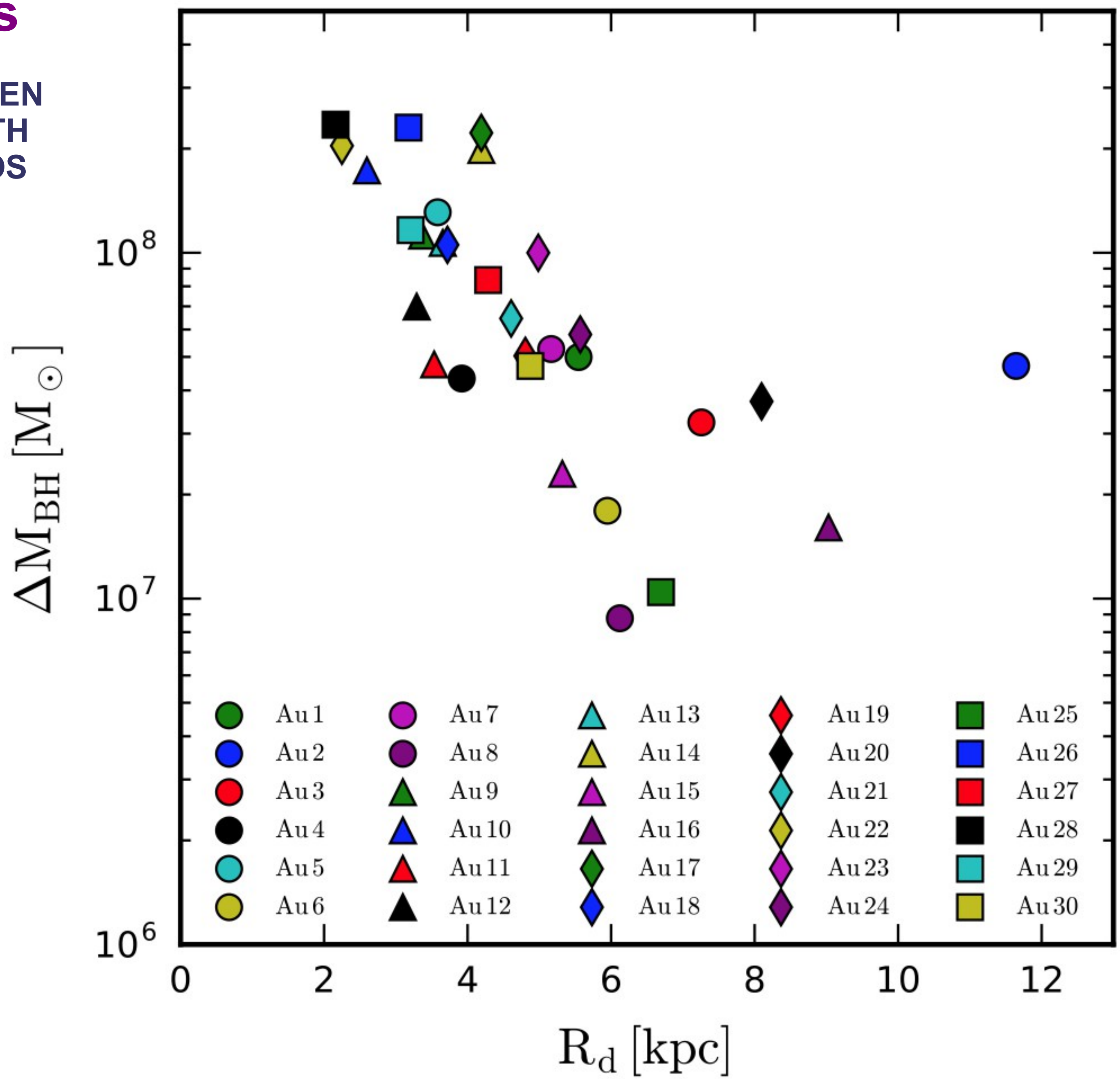

Grand et al. (2016)

The sizes of different galaxies types reproduce observed trends with stellar mass well

ILLUSTRIS-TNG GALAXY SIZES AS A FUNCTION OF STELLAR MASS

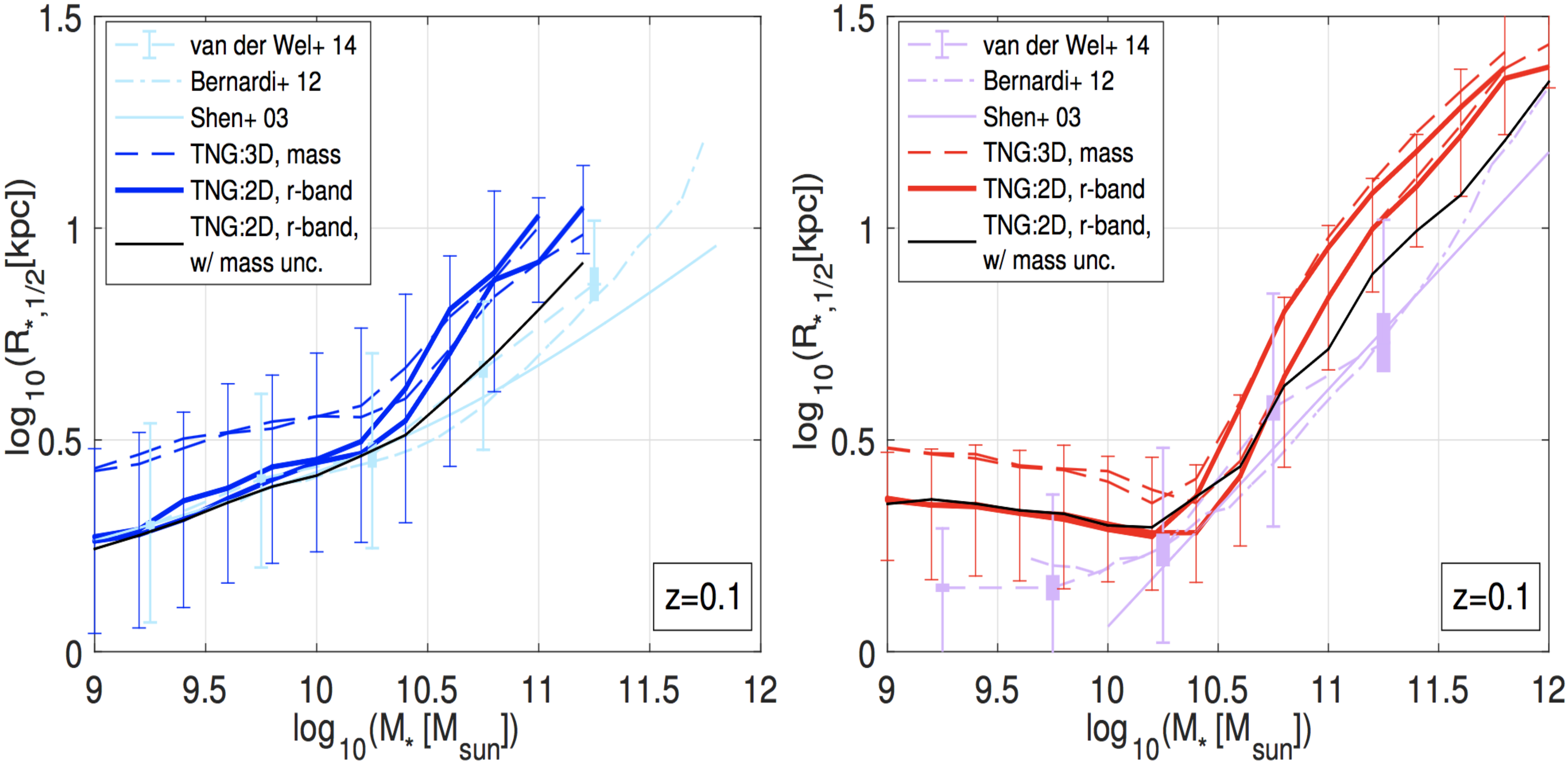

(a) Main-sequence / late-type galaxies

(b) Quenched / early-type galaxies

Genel et al. (2018)

Observed metallicity profiles of galaxy clusters are reproduced by IllustrisTNG

METALLICITY MAPS AND PROFILES FOR RICH GALAXY CLUSTERS

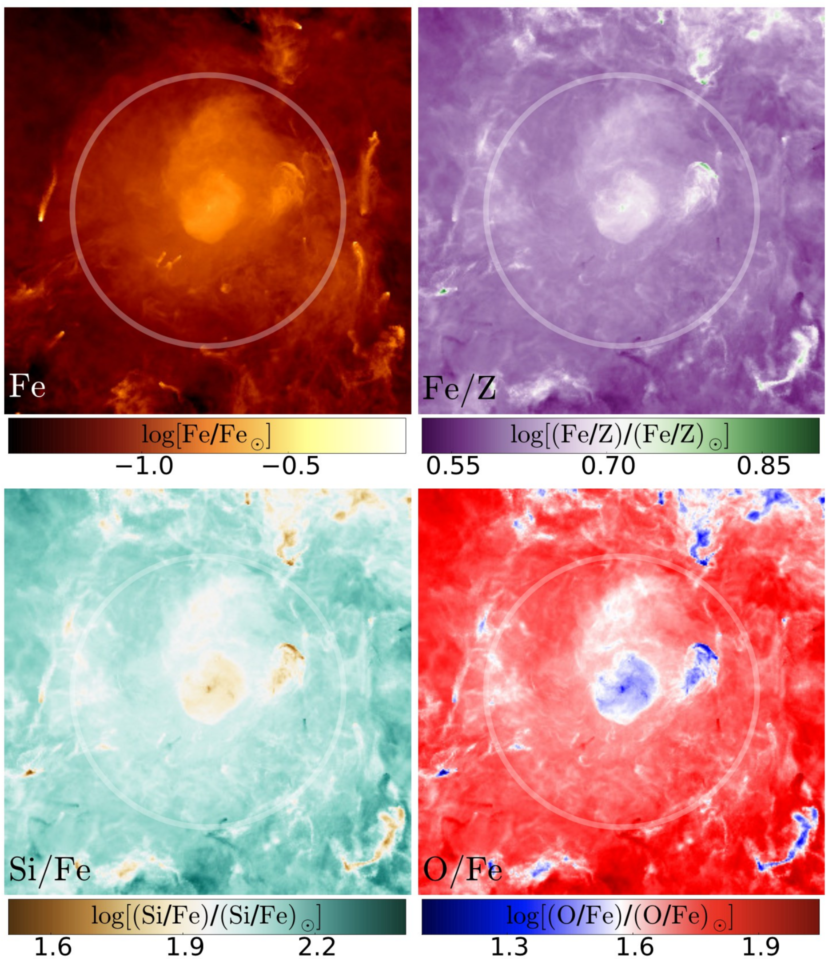

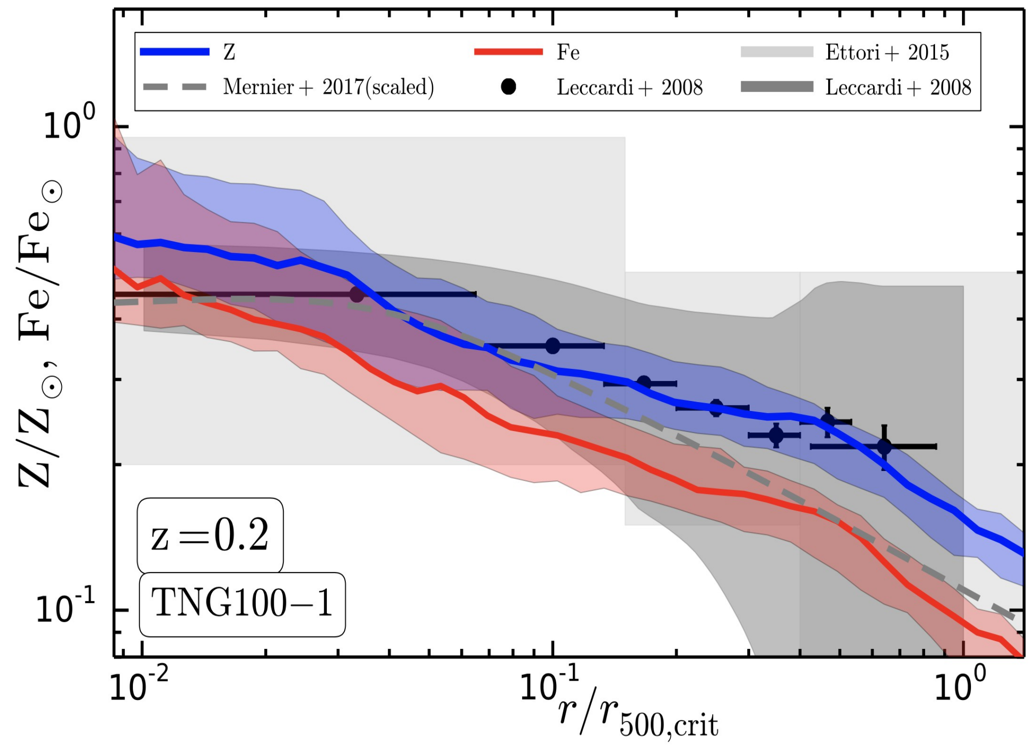

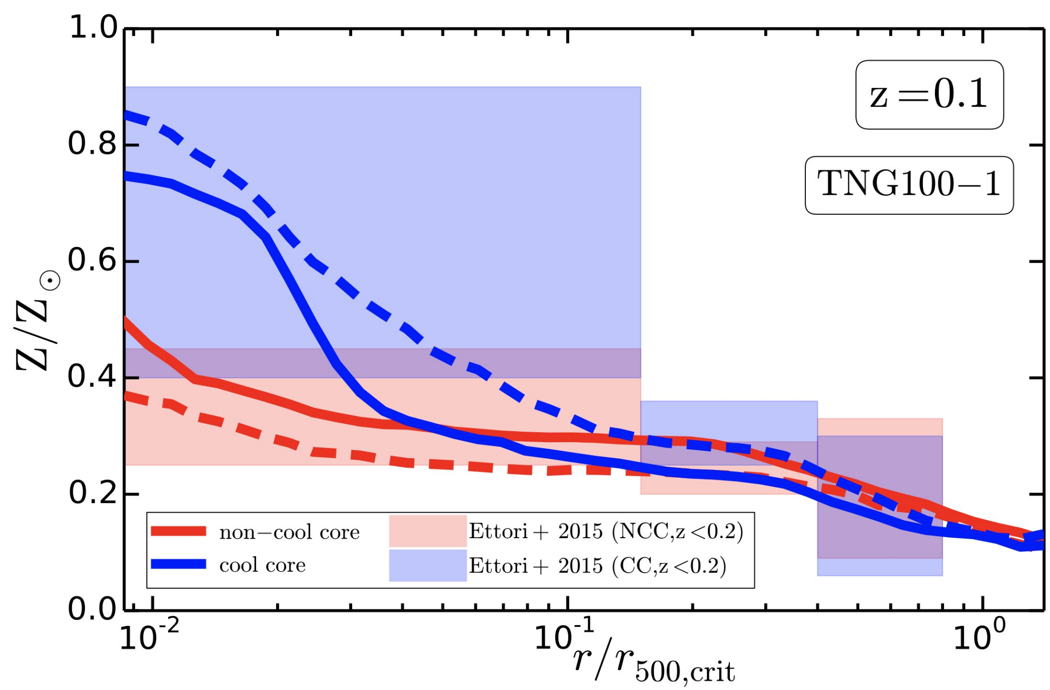

Vogelsberger et al. (2017)

Magnetic field
results

Our MHD simulations of galaxy formation predict the amplification of primordial fields in halos and galaxies

MAGNETIC FIELD STRENGTH IN A SMALL REGION OF ILLUSTRIS-TNG

The IllustrisTNG simulations predict the magnetic field strength and field topology in galaxies

STELLAR MASS, GAS DENSITY AND MAGNETIC FIELD STRENGTH IN A TYPICAL SPIRAL

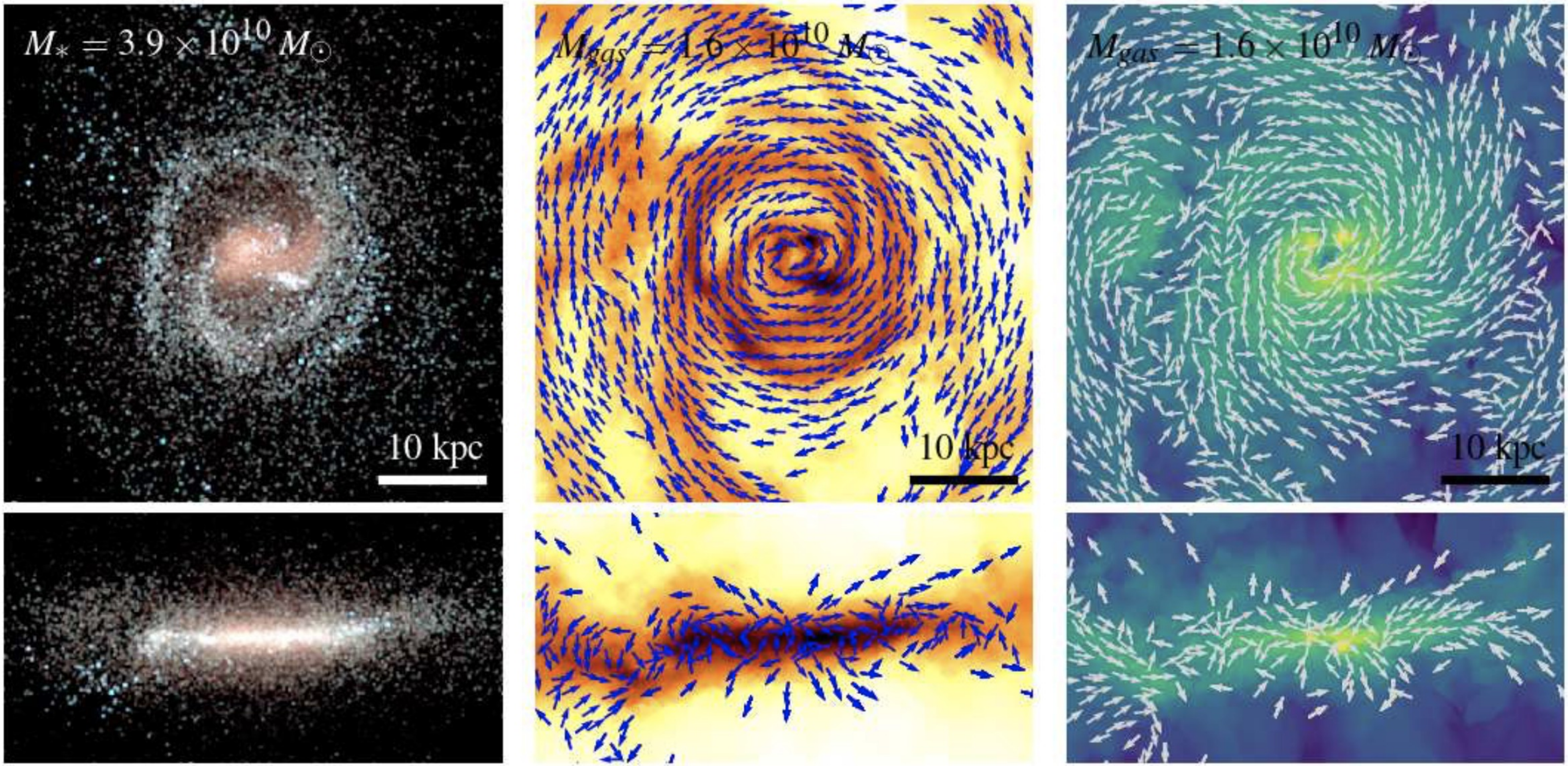

Marinacci et al. (2018)

The AURIGA simulations yield disk galaxies with stellar mass and spatial structure consistent with Milky Way-like galaxies

FACE-ON STELLAR MASS DENSITY PROJECTIONS OF TWO SIMULATIONS FROM THE AURIGA SUITE

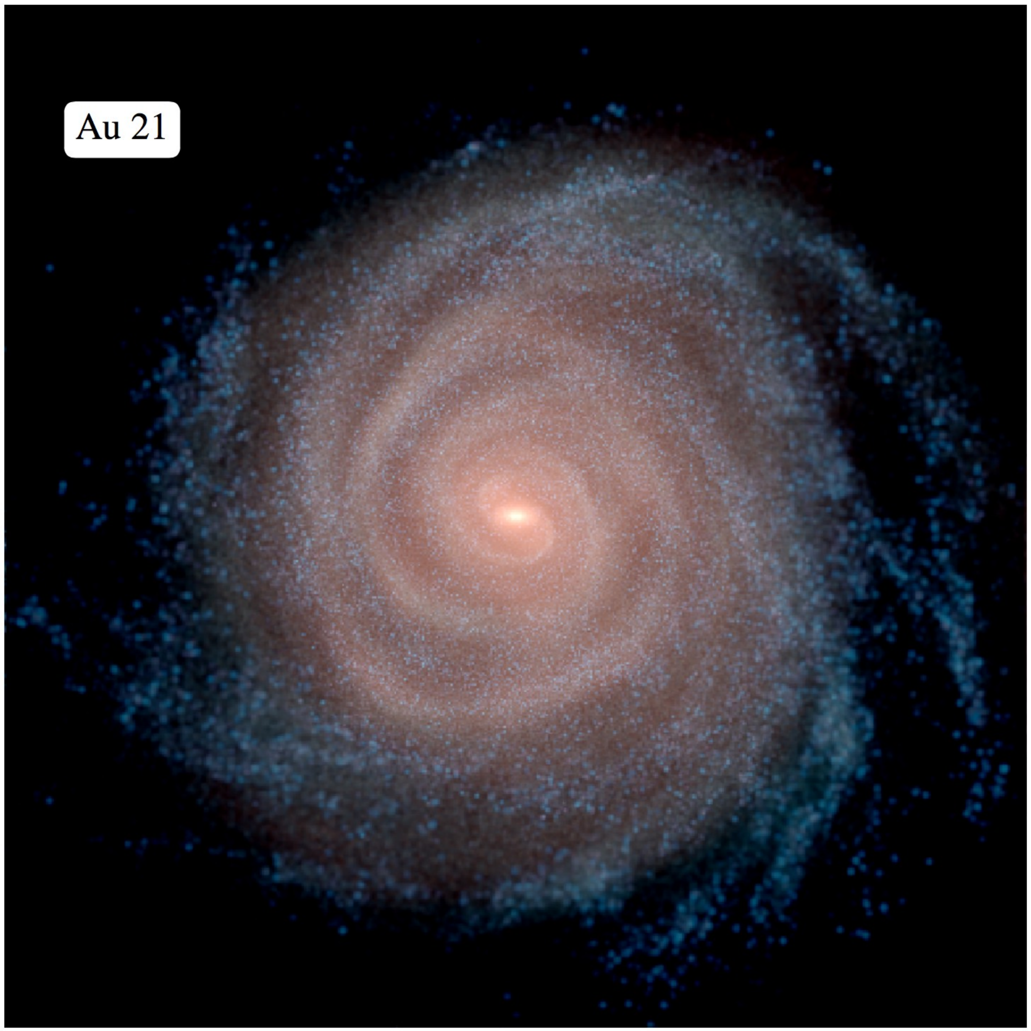

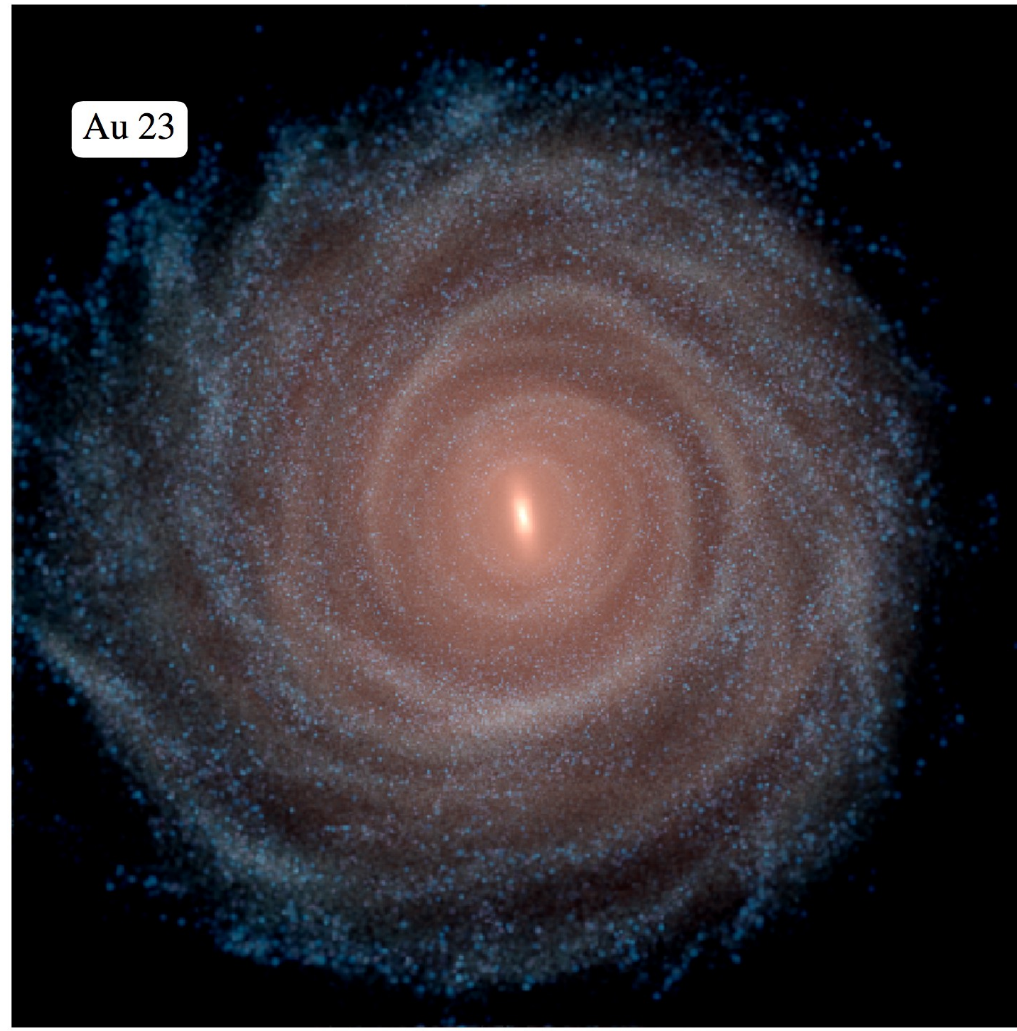

Grand, Springel, Pakmor, et al. (2017)

A small-scale dynamo is active at very high redshift

EVOLUTION OF THE VOLUME-WEIGHTED RMS B-FIELD STRENGTH INSIDE 10 KPC

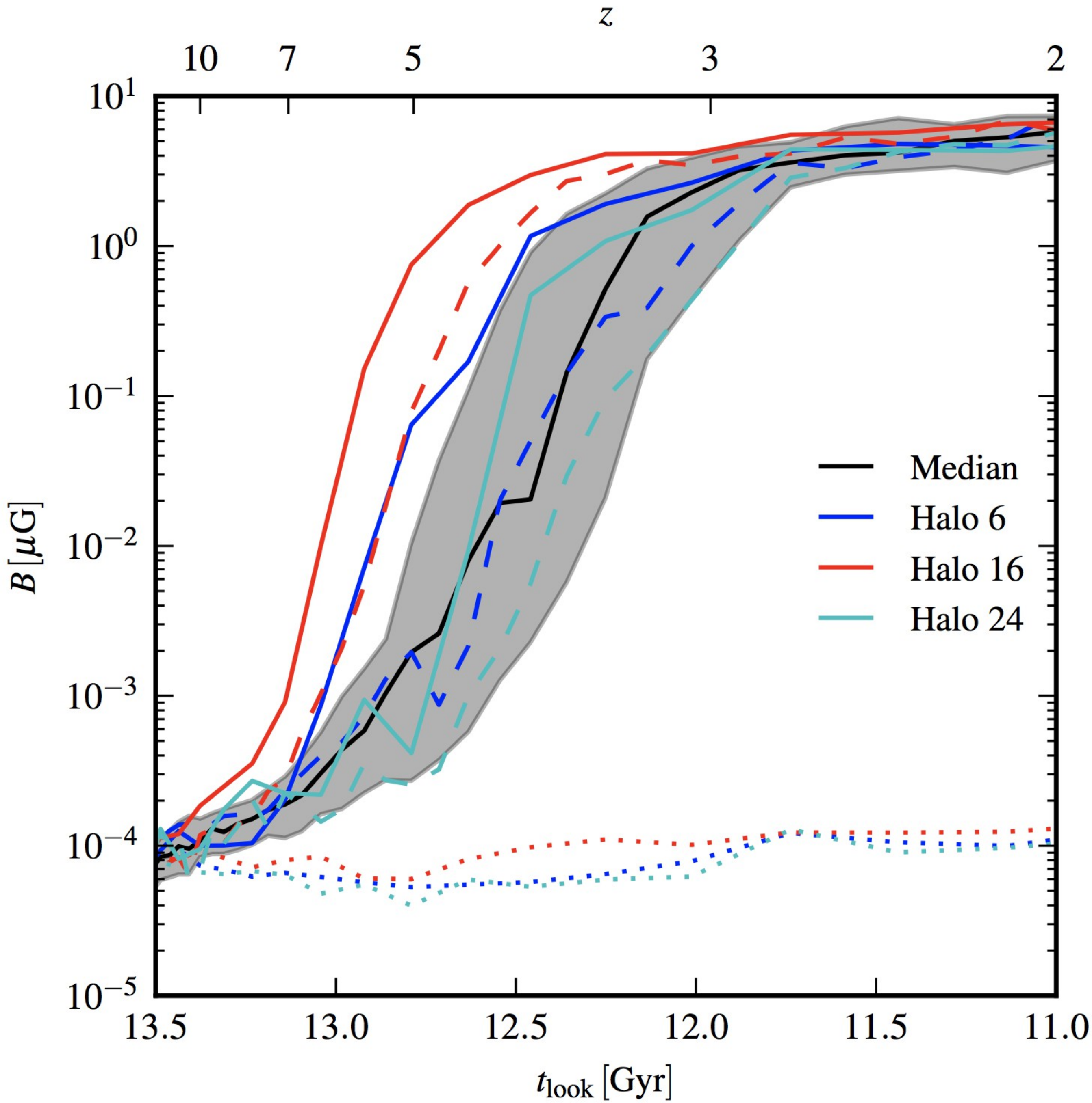

Pakmor et al. (2017)

Amplification of B-field occurs through turbulent dynamo

VELCOITY FIELD AND EVOLUTION OF VELOCITY AND B-FIELD POWER SPECTRA

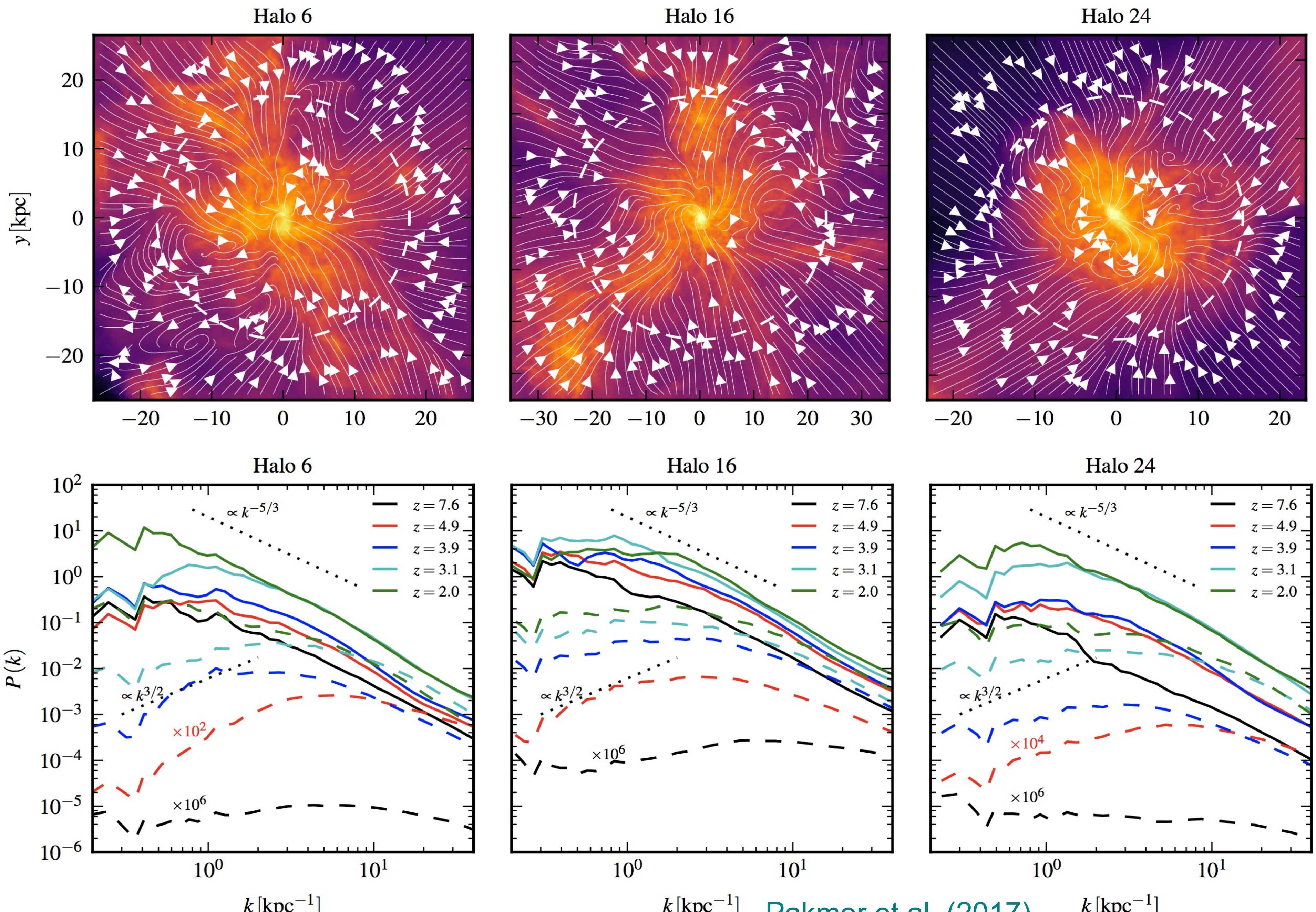

Pakmor et al. (2017)

The predicted magnetic field strength agrees quite well with observations

PROFILES OF MAGNETIC FIELD STRENGTH IN SIMULATIONS AND OBSERVATIONS

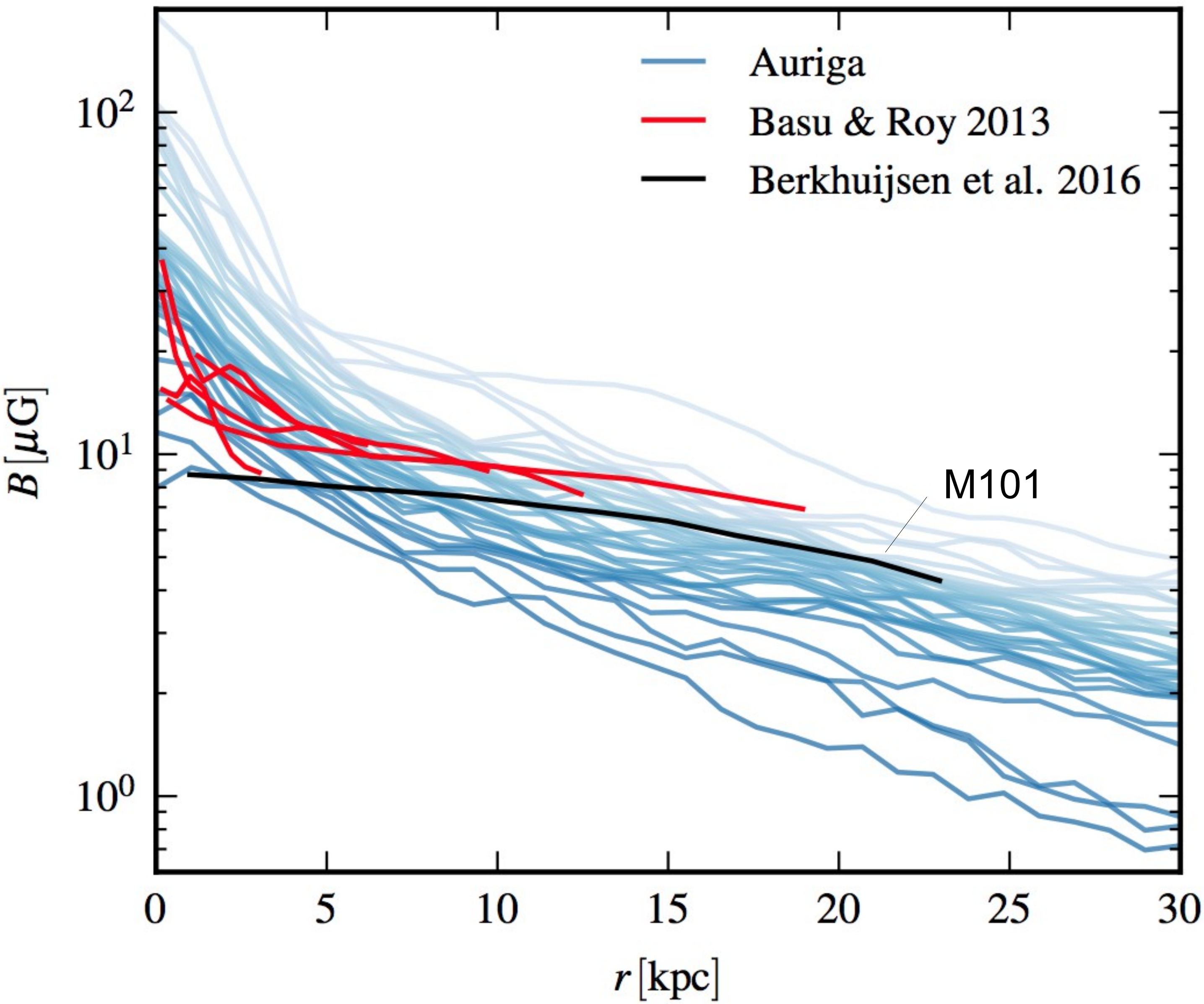

Pakmor et al. (2017)

Cosmic rays and their impact on galactic outflows

In isolated disk galaxy formation simulations, magnetic fields drive magnetically driven small fountain like flows out of the disk

SLICES THROUGH THE GAS DENSITY AND THE MAGNETIC FIELD

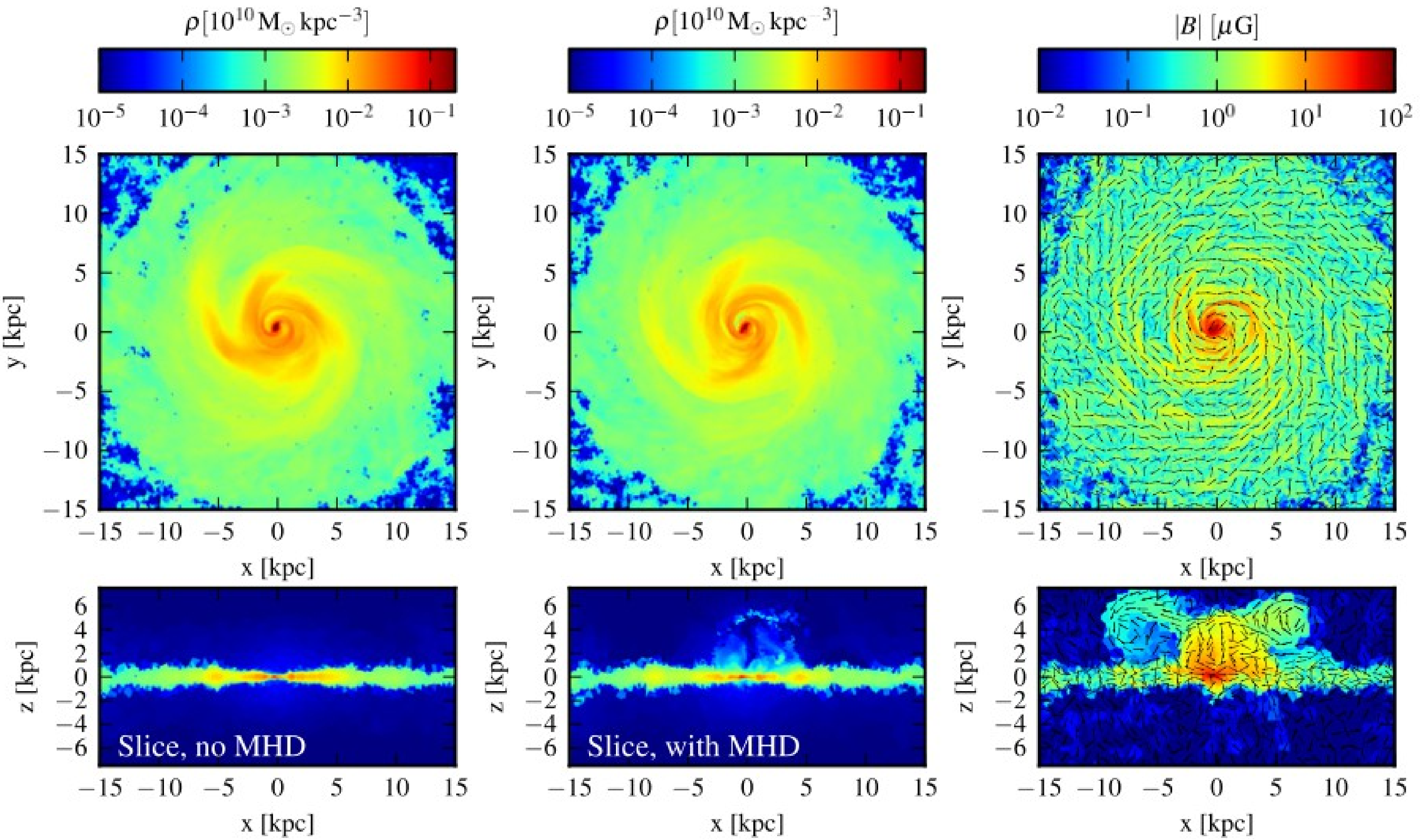

Pakmor & Springel (2012)

The CR dynamics is coupled to magnetic fields permeating the gas

INTERACTIONS OF COSMIC RAYS AND MAGNETIC FIELDS

Cosmic rays scatter on magnetic fields – this lets them exert a pressure on the thermal gas, and diffuse relative to its rest frame.

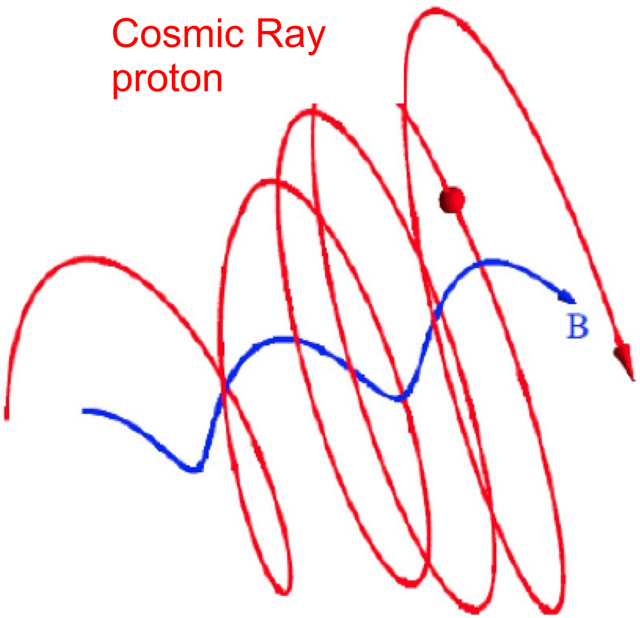

Streaming instability:

- CRs can in principle move rapidly along field lines (with c), which acts to reduce any gradient in their number density.
- But if $c_s > v_A$, CR excite Alfven waves (streaming instability)
- scattering off this wave field in turn limits the CR bulk speed to a much smaller, effective streaming speed v_{str}
- streaming speed: $$\mathbf{v}_{\rm str} = -v_{\rm str}\frac{\nabla P_{\rm cr}}{|\nabla P_{\rm cr}|}$$ $$v_{\rm str} = \lambda\,\max(c_S, v_A)$$ $$\lambda \sim 1$$

The CR transport complicates fluid dynamics considerably

COSMIC RAY DYNAMICS WITHOUT SOURCE AND SINK TERMS

$$\frac{\partial \boldsymbol{U}}{\partial t} + \boldsymbol{\nabla} \cdot \mathbf{F} = \boldsymbol{S}$$

$$\boldsymbol{U} = \begin{pmatrix} \rho \\ \rho \boldsymbol{v} \\ \varepsilon \\ \varepsilon_{\mathrm{cr}} \\ \boldsymbol{B} \end{pmatrix}, \quad \mathbf{F} = \begin{pmatrix} \rho \boldsymbol{v} \\ \rho \boldsymbol{v}\boldsymbol{v}^{\mathrm{T}} + P\mathbf{1} - \boldsymbol{B}\boldsymbol{B}^{\mathrm{T}} \\ (\varepsilon + P)\boldsymbol{v} - \boldsymbol{B}\,(\boldsymbol{v} \cdot \boldsymbol{B}) \\ \varepsilon_{\mathrm{cr}}\boldsymbol{v} + (\varepsilon_{\mathrm{cr}} + P_{\mathrm{cr}})\boldsymbol{v}_{\mathrm{st}} - \kappa_{\varepsilon}\boldsymbol{b}\,(\boldsymbol{b} \cdot \boldsymbol{\nabla}\varepsilon_{\mathrm{cr}}) \\ \boldsymbol{B}\boldsymbol{v}^{\mathrm{T}} - \boldsymbol{v}\boldsymbol{B}^{\mathrm{T}} \end{pmatrix}, \quad \boldsymbol{S} = \begin{pmatrix} 0 \\ \mathbf{0} \\ P_{\mathrm{cr}}\,\boldsymbol{\nabla} \cdot \boldsymbol{v} - \boldsymbol{v}_{\mathrm{st}} \cdot \boldsymbol{\nabla} P_{\mathrm{cr}} + \Lambda_{\mathrm{th}} + \Gamma_{\mathrm{th}} \\ -P_{\mathrm{cr}}\,\boldsymbol{\nabla} \cdot \boldsymbol{v} + \boldsymbol{v}_{\mathrm{st}} \cdot \boldsymbol{\nabla} P_{\mathrm{cr}} + \Lambda_{\mathrm{cr}} + \Gamma_{\mathrm{cr}} \\ \mathbf{0} \end{pmatrix}$$

$$P = P_{\mathrm{th}} + P_{\mathrm{cr}} + \frac{\boldsymbol{B}^2}{2} \qquad \varepsilon = \varepsilon_{\mathrm{th}} + \frac{\rho \boldsymbol{v}^2}{2} + \frac{\boldsymbol{B}^2}{2} \qquad \boldsymbol{v}_{\mathrm{st}} = -\frac{\boldsymbol{B}}{\sqrt{\rho}}\,\mathrm{sgn}(\boldsymbol{B} \cdot \boldsymbol{\nabla} P_{\mathrm{cr}})$$

cosmic ray streaming,
nasty(!) numerically

Energy equation:

$$\frac{\partial \varepsilon_{\mathrm{cr}}}{\partial t} + \boldsymbol{\nabla} \cdot \left[\varepsilon_{\mathrm{cr}}(\boldsymbol{v} + \boldsymbol{v}_{\mathrm{st}}) - \kappa_{\varepsilon}\boldsymbol{b}\,(\boldsymbol{b} \cdot \boldsymbol{\nabla}\varepsilon_{\mathrm{cr}})\right] = -P_{\mathrm{cr}}\,\boldsymbol{\nabla} \cdot (\boldsymbol{v} + \boldsymbol{v}_{\mathrm{st}}) + \Lambda_{\mathrm{cr}} + \Gamma_{\mathrm{cr}}$$

anisotropic diffusion

Transport processes of CRs are critical for driving galactic winds

COMPARISON OF DISK GALAXY EVOLUTION WITH DIFFERENT COSMIC RAY PHYSICS

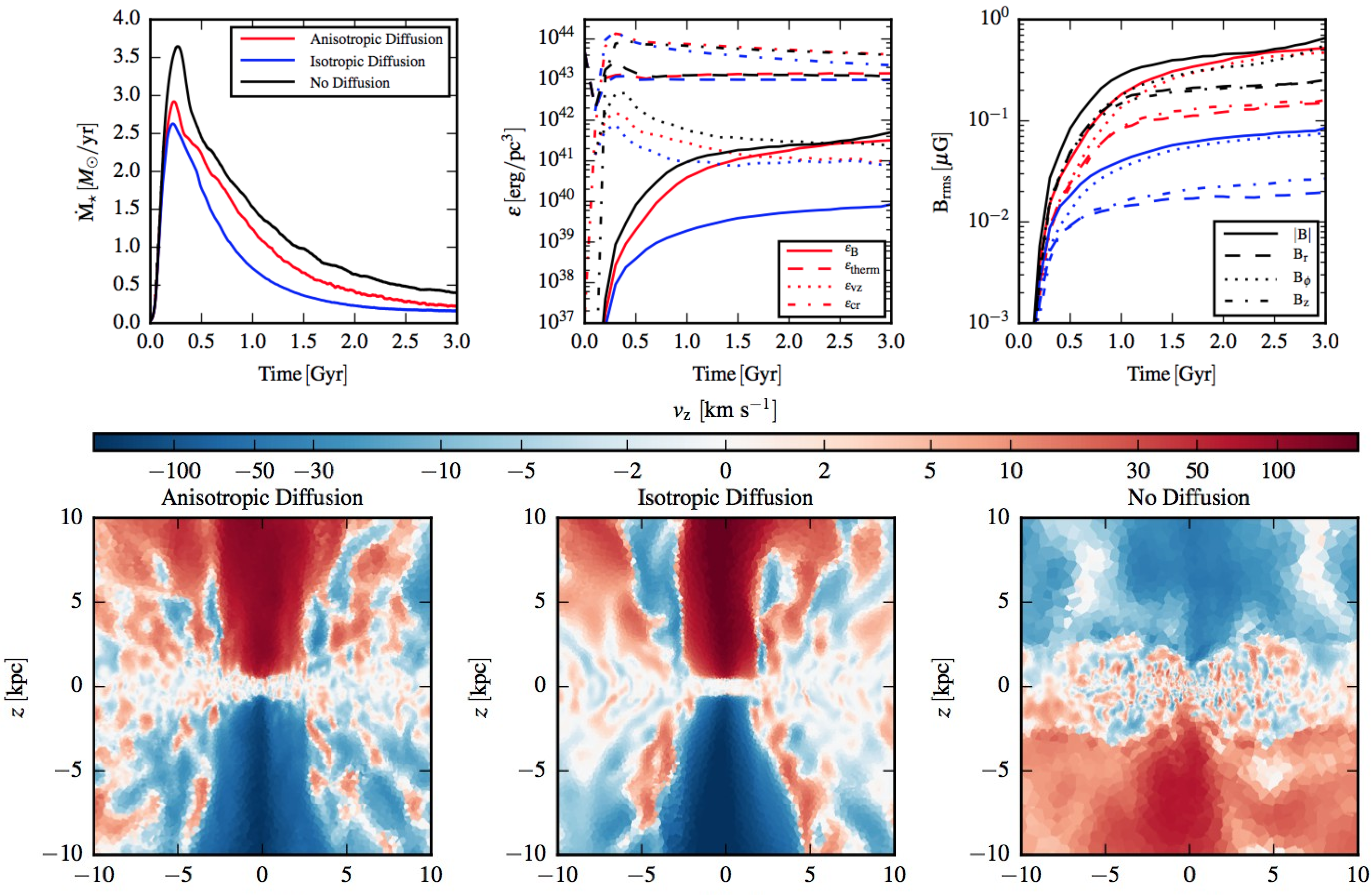

Pakmor et al. (2016)

The efficiency of cosmic ray driven winds is a strong function of halo mass

Jacob et al. (2017)

OUTFLOW VELOCITIES IN ISOLATED GALAXIES OF DIFFERENT SIZE

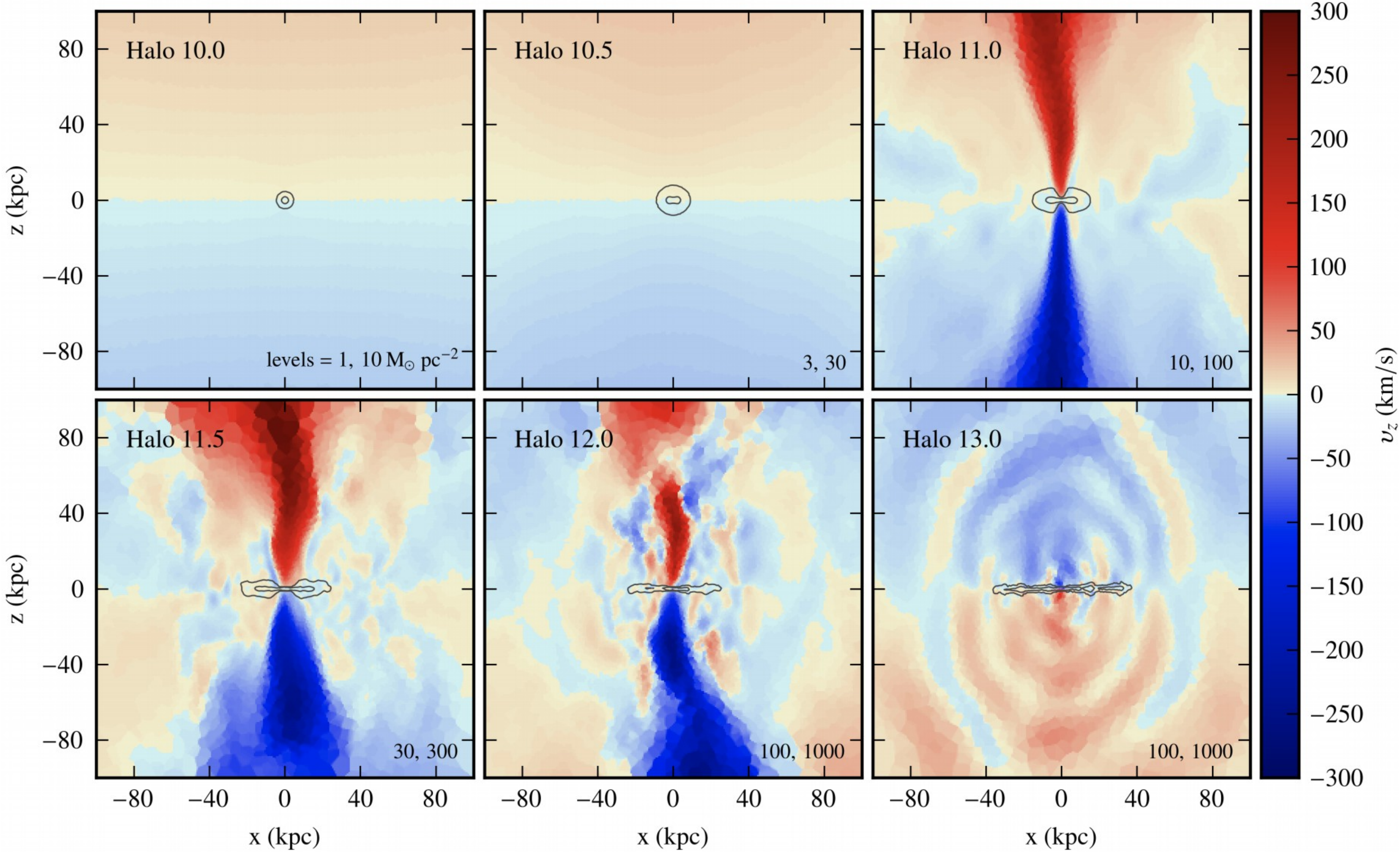

The mass loading of CR-driven winds depends strongly on halo mass, whereas the energy loading is flat

PROPERTIES OF CR DRIVEN WINDS AS A FUNCTION OF HALO MASS

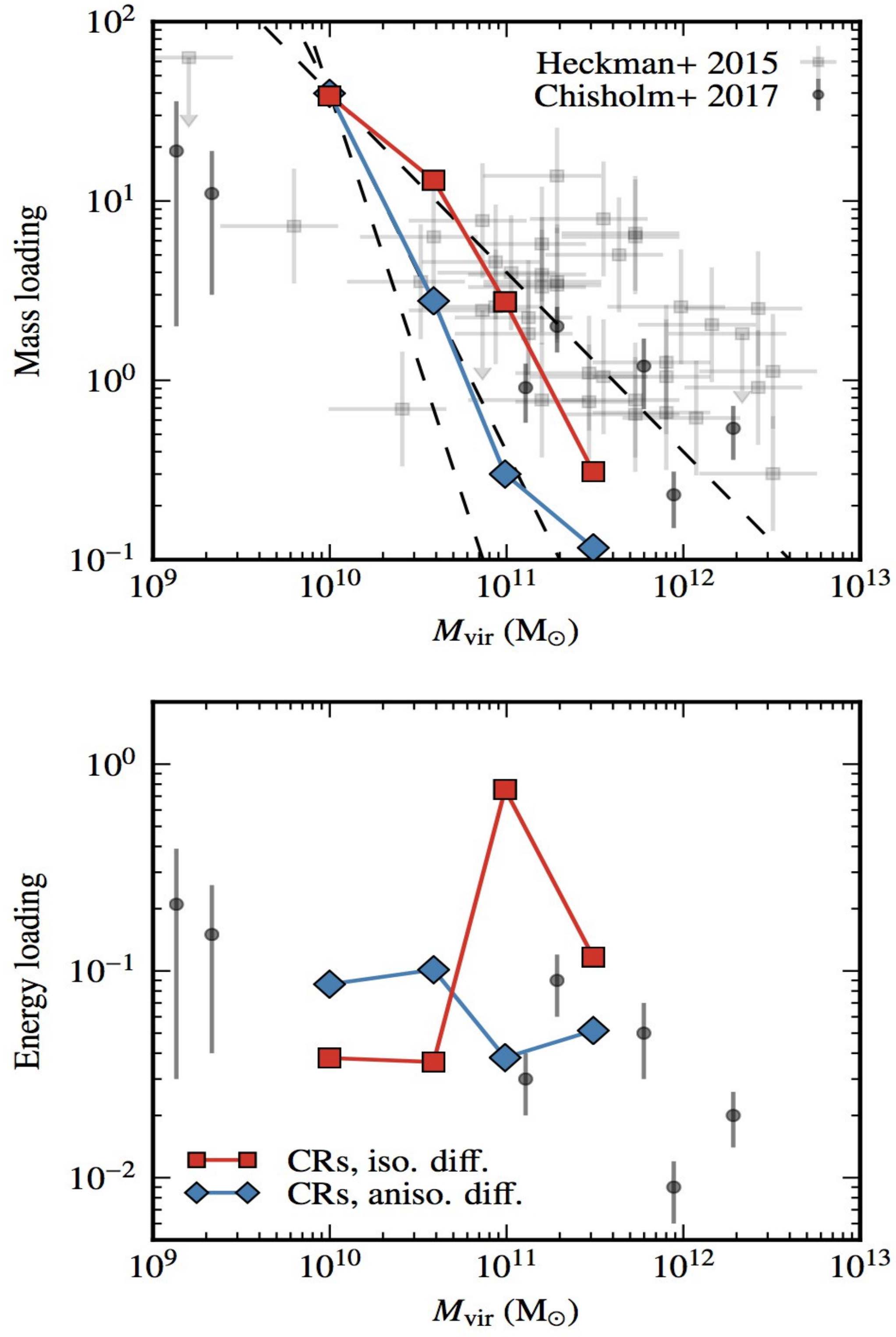

Jacob et al. (2017)

The unknown CR diffusion constant and injection efficiency represent important uncertainties

MASS LOADING OF CR-DRIVEN WINDS FOR DIFFERENT MODEL PARAMETERS

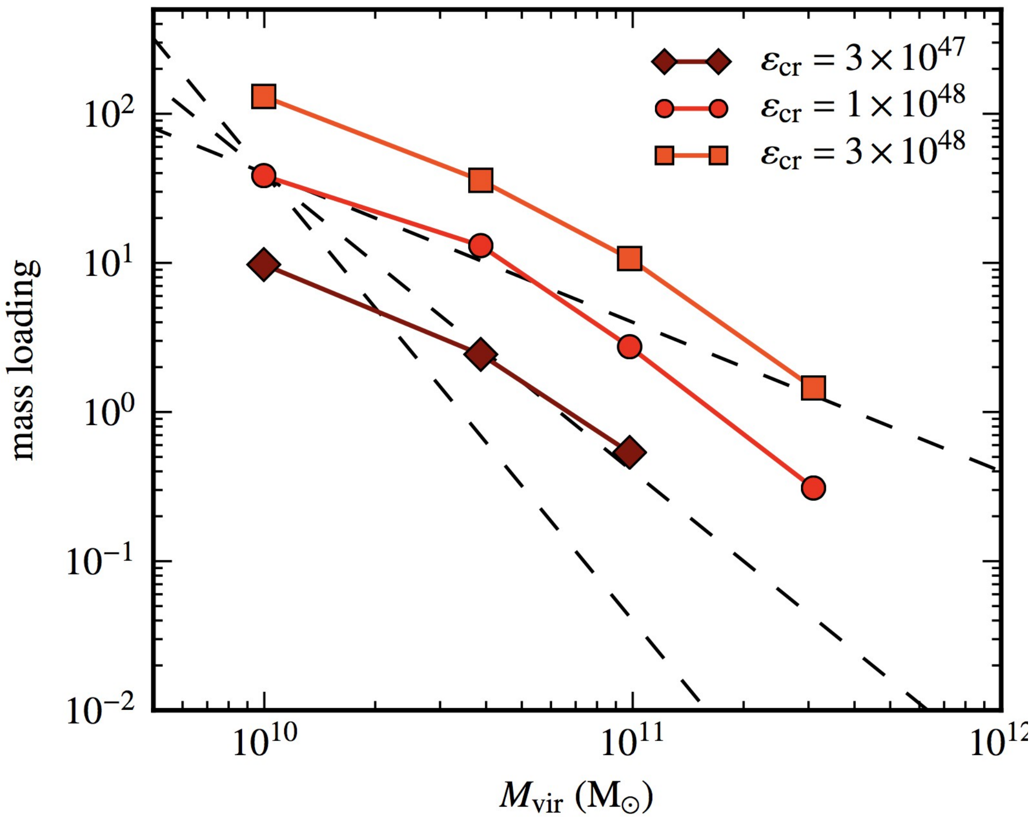

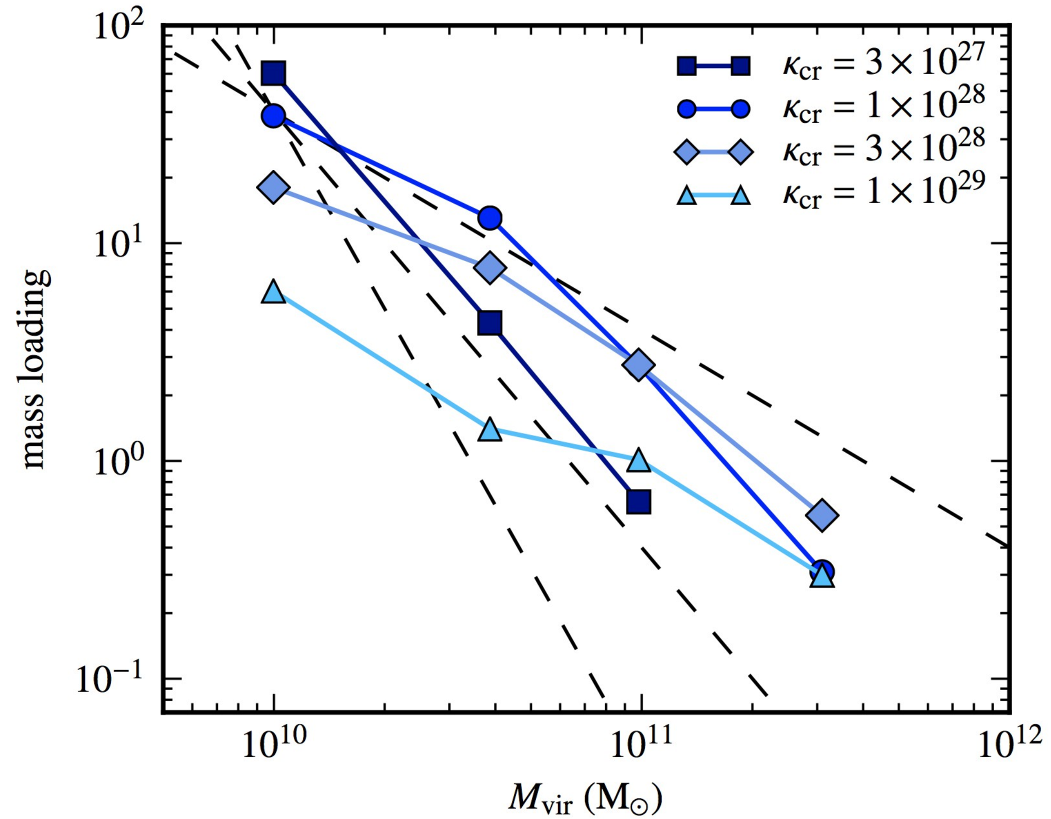

Jacob et al. (2017)

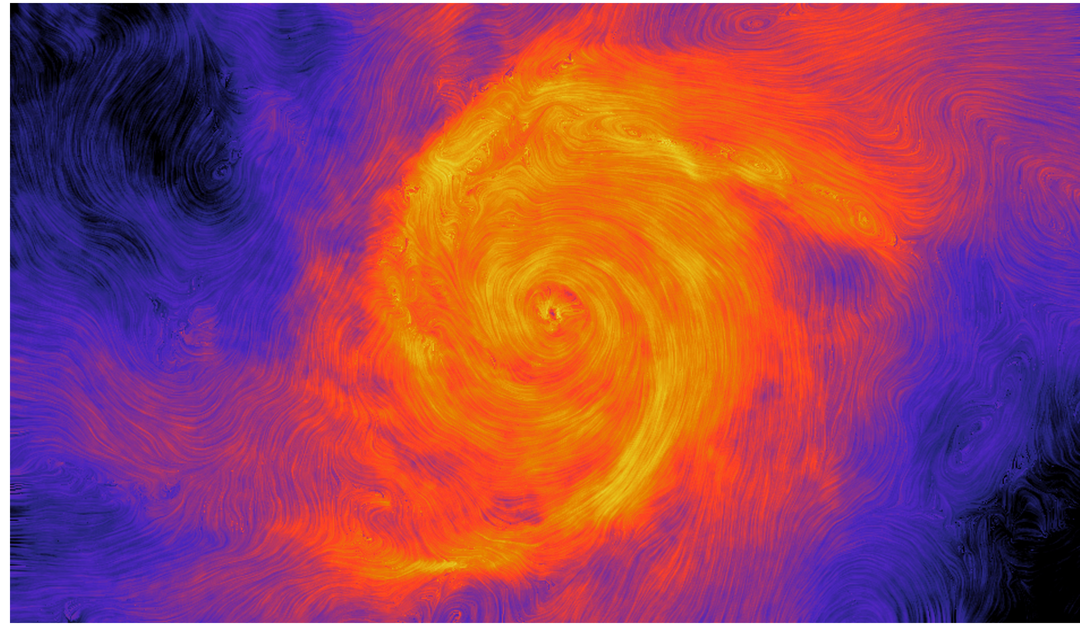

Take home points

- **Hydrodynamic cosmological simulations** of ΛCDM can now quite **successfully predict galaxy morphologies, clustering, and quenching**, as well as diffuse gas properties in the CGM, IGM, and ICM, from high-z to the present
- **Black hole feedback** processes are critical for galaxy formation and evolution
- A **small-scale dynamo driven by** feedback generated **turbulence** can efficiently amplify tiny seed fields already at high redshift to the observed strength
- **Cosmic rays** may play a key role in explaining **galactic outflows**